

The Galilean Satellites: An Overview

Channon Visscher

Dordt University, Sioux Center, Iowa 51250, USA

Space Science Institute, Boulder, Colorado, 80301, USA

channon.visscher@dordt.edu

preprint for *The Oxford Research Encyclopedia of Planetary Science*

September 17, 2025

Abstract

The four largest moons of Jupiter—Io, Europa, Ganymede, and Callisto—are known as the Galilean satellites, named after Galileo Galilei, who discovered them in 1610. Early 19th-century observations revealed that the three inner moons are locked in a 4:2:1 Laplacian orbital resonance, a relationship that has had significant implications for their internal heating and subsequent thermal evolution. By the dawn of the space age, the bulk densities and major surface components of the Galilean satellites had been measured, showing planetary-mass bodies that offer striking examples of how variations in composition, orbital dynamics, and geologic processes can lead to dramatically different surface expressions. Their bulk compositions vary with distance from Jupiter: Io and Europa are denser and dominated by rock, while Ganymede and Callisto show increasing proportions of water ice. Io is the most volcanically active body in the Solar System – a consequence of intense tidal heating – and exhibits high-temperature mafic volcanism amid a sulfur-coated surface. Neutral atoms escaping from Io’s surface also supplies material to the broader Jovian system environment. Europa is enveloped in a smooth icy shell overlying a global subsurface ocean, with surface features that hint at exchange between the ocean and surface and the possibility of plumes of water erupting above the icy surface. Ganymede and Callisto, both composed of rock and ice, diverge markedly in

their geologic histories: Ganymede shows evidence of tidal heating, tectonic resurfacing, and a magnetic field, while Callisto's surface is dominated by ancient impact craters – suggestive of minimal internal evolution and partial differentiation – but also shows a process of sublimation and degradation that destroys surface features at small scales. Much of our current understanding of the Galilean system comes from telescopic observations and spacecraft missions, notably the *Voyager 1* and *Voyager 2* encounters in 1979 and the *Galileo* orbiter, which completed 34 orbits of Jupiter over a seven-year mission from 1995-2003. Together, the Galilean moons serve as natural laboratories for comparative planetology, illustrating diverse processes such as thermal and internal evolution, surface tectonics, impact cratering, and surface-atmosphere-space environment interactions. Ongoing exploration and upcoming spacecraft missions aim to further investigate the geological diversity of these worlds, as well as the chemical and potential biological significance of subsurface oceans on Europa, Ganymede, and possibly Callisto.

Keywords: planetary satellites; satellite interiors; satellite surfaces; Jupiter system; Galilean moons; Io; Europa; Ganymede; Callisto

³⁹ **1 History of Observations**

⁴⁰ **1.1 From 1610 to the space age**

⁴¹ The four largest moons of Jupiter – Io, Europa, Ganymede, and Callisto – were first observed
⁴² by Galileo Galilei in January 1610. Taking them at first to be stars, Galileo soon realized that
⁴³ what he named (in a nod to his patrons) the “Medicean planets” were in orbital revolution around
⁴⁴ Jupiter. His observations of their positions over the next several weeks, recorded in the landmark
⁴⁵ *Sidereus Nuncius* (Galilei 1610), would provide a powerful demonstration against a geocentric un-
⁴⁶ derstanding of the universe and played a significant role as evidence – as the first objects orbiting
⁴⁷ a planet other than the Earth – in favor of a heliocentric or Copernican view of the cosmos. These
⁴⁸ four moons are now collectively known as the Galilean satellites. Their individual names, how-
⁴⁹ ever, were first proposed in *Mundus Jovialis* by Simon Marius in 1614, who reported independent
⁵⁰ observations of these moons in late 1609 and early 1610 (see Prickard 1916).

⁵¹ Galileo would later record orbital periods of 1.77 days (Io), 3.56 d (Europa), 7.17 d (Ganymede)
⁵² and 16.75 d (Callisto), very close to the values reported by Marius (Prickard 1916) and to the
⁵³ modern values of 1.769, 3.551, 7.155, and 16.689 d, respectively. However, Pierre Simon Laplace
⁵⁴ was the first to describe and demonstrate the stability of the 4:2:1 mean motion resonance between
⁵⁵ Io, Europa, and Ganymede in detail (Laplace 1805): for every one orbit of Ganymede, Europa
⁵⁶ completes 2 orbits and Io completes 4 orbits. The Laplace relation can also be expressed as

$$\lambda_1 - 3\lambda_2 - 2\lambda_3 \approx 180^\circ \quad (1)$$

⁵⁷ where λ_1 , λ_2 , and λ_3 refer to the mean orbital longitude of Io, Europa, and Ganymede, respectively.
⁵⁸ This so-called Laplacian resonance would become the subject of intense study and analysis over
⁵⁹ the following centuries, including in the construction of increasingly precise satellite ephemerides.
⁶⁰ It also allowed for the first characterization of the physical properties of the Galilean satellites
⁶¹ themselves. For example, analysis of the mutual orbital perturbations of the satellites provided
⁶² the first estimates of satellite masses (e.g., see Aksnes 1977; Greenberg 1977; Pollack & Fanale
⁶³ 1982), including an early estimate by Laplace (1805). Later treatments based upon improved
⁶⁴ observations would deduce satellite masses to within 5% of modern values for Io, Europa, and

65 Ganymede (Sampson 1921) and Europa and Ganymede (de Sitter 1931). A summary of mass
 66 estimates and measurements is given in Table 1.

Source/Author	Io	Europa	Ganymede	Callisto
Laplace (1805)	1.73×10^{-5}	2.32×10^{-5}	8.85×10^{-5}	4.27×10^{-5}
Sampson (1921)	4.50×10^{-5}	2.54×10^{-5}	7.99×10^{-5}	4.50×10^{-5}
de Sitter (1931)	3.81×10^{-5}	2.48×10^{-5}	8.17×10^{-5}	5.09×10^{-5}
Pioneer 10 (Anderson <i>et al.</i> 1974)	4.70×10^{-5}	2.57×10^{-5}	7.85×10^{-5}	5.60×10^{-5}
Galileo (Anderson <i>et al.</i> 1996a,b, 1997a,b)	4.704×10^{-5}	2.528×10^{-5}	7.805×10^{-5}	5.667×10^{-5}

Table 1: Galilean satellite masses relative to Jupiter ($M_J = 1.8986 \times 10^{27}$ kg). After Table 3.2 in Aksnes (1977). Values for Laplace (1805) are taken from the compilation of Houzeau (1882).

67 The earliest measurements of the diameters of the Galilean satellites involved timing the du-
 68 ration of their entry into Jupiter’s shadow (e.g., Cassini 1693) or in front of Jupiter’s disk (e.g.,
 69 Herschel 1797) (incidentally, careful study of the timing between Io eclipse events allowed Danish
 70 astronomer Ole Rømer to establish that light has a finite velocity; e.g. Bobis & Lequeux 2008).
 71 Early eclipse observations tended to over-estimate the sizes of the Galilean moons by 50%-100%
 72 (for a compilation of early diameter measurements, see Houzeau 1882). Diameter measurements
 73 would significantly improve with increasing telescope sizes throughout the late 18th and 19th cen-
 74 turies (Houzeau 1882), along with the use of the filar micrometer, which allowed for direct mea-
 75 surements of angular diameters (e.g., Secchi 1856; Webb 1871; Barnard 1895). By the late 19th
 76 century, Galilean satellite diameters had been measured to within 10% of modern values (see Mor-
 77 rison *et al.* 1977). Prior to spacecraft exploration of the Jupiter system, highly precise diameter
 78 measurements were also obtained by stellar occultation observations of Io (of β Scorpii C on 14
 79 May 1971; Taylor 1972) and Ganymede (of SAO 186800 on 7 June 1972; Carlson *et al.* 1973).

80 Measurements of both the masses and diameters of the Galilean satellites allowed for initial
 81 estimates of their mean densities, a fundamental parameter for inferring bulk composition. Io (3.5
 82 g/cm³) and Europa (3.0 g/cm³) have densities roughly similar to that of the Moon (3.3 g/cm³),
 83 whereas Ganymede (1.9 g/cm³) and Callisto (1.8 g/cm³) have much lower densities. The observed
 84 density trend suggests bulk compositions for Io and Europa characterized by a significant rocky
 85 component, with a increasing proportion of water ice moving outward to Ganymede and Callisto.
 86 This trend is generally attributed to conditions present in the proto-Jupiter circumplanetary disk
 87 during the time of satellite formation.

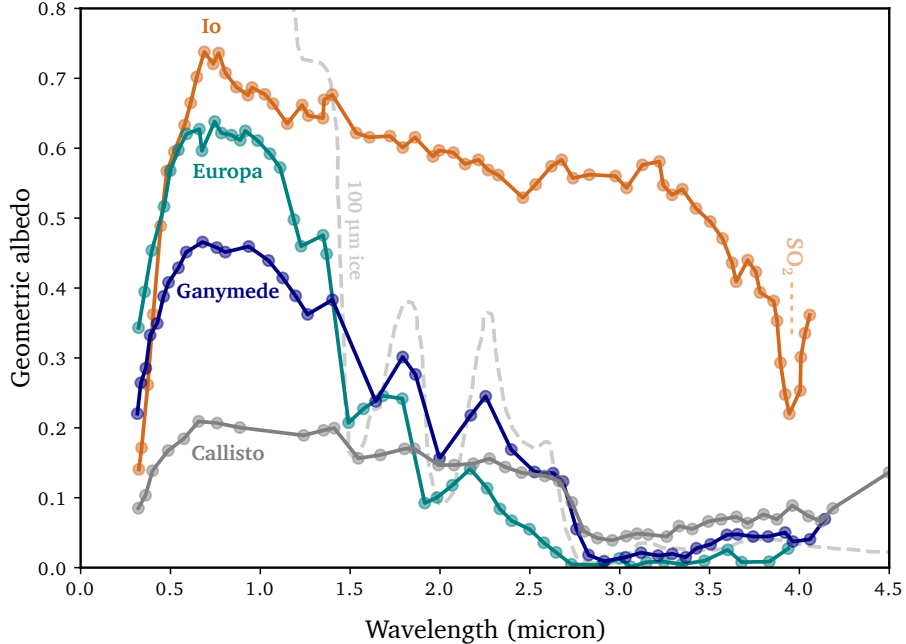


Figure 1: Near-infrared reflectance spectra (as geometric albedo) of the Galilean satellites based upon telescopic observations. Also shown for reference is the SO_2 absorption band at $4\text{-}\mu\text{m}$ and the calculated reflectance of water ice with $100\text{-}\mu\text{m}$ grain size (Calvin *et al.* 1995). Modified after Johnson (2014) based upon the compilation Clark & McCord (1980) (cf. Pollack *et al.* 1978; McFadden *et al.* 1980; Sill & Clark 1982; Lebofsky & Feierberg 1985; Calvin *et al.* 1995).

Comparisons of visual magnitudes and diameter measurements could also be used to provide information about surface properties. For example, Pickering *et al.* (1879) combined the micrometer diameter measurements of R. Engelmann with photometric measurements to estimate albedo values roughly similar (and consistent in trend) to modern values. The first photoelectric measurements of the surface were taken by Stebbins (1927) and Stebbins & Jacobsen (1928) using a quartz-potassium cell. By the mid-20th century, improvements in visible and infrared spectrophotometric techniques and the use of larger telescopes provided more detailed observations of the disk-integrated properties of the Galilean surfaces (e.g., see reviews by Harris 1961; Morrison *et al.* 1977; Johnson & Pilcher 1977; Morrison 1982; Sill & Clark 1982). Near-infrared reflectance spectra of the Galilean satellites from telescopic observations are summarized in Figure 1. Based upon near-infrared photometry, Kuiper (1957) and Moroz (1961) proposed that Europa and Ganymede had surfaces covered by water ice, where the lower albedo of Ganymede could be explained by ice possibly “contaminated with silicate dust” (Kuiper 1957). The presence of water ice on Europa, Ganymede, and Callisto was confirmed by infrared spectroscopic observations by Pilcher

102 *et al.* (1972) and (Fink *et al.* 1973). Meanwhile, spectrophotometric observations continued to
 103 demonstrate the high albedo of Io, its reddish color, and the apparent absence of water ice (Morri-
 104 son 1982), and UV spectra suggested the presence of sulfur-bearing compounds (Wamsteker *et al.*
 105 1974) such as SO₂ frost (Fanale *et al.* 1979; Clark & McCord 1980; Sill & Clark 1982). Ground-
 106 based observations also demonstrated sodium emission from the vicinity of Io (Brown & Chaffee
 107 1974), providing early clues to the chemical composition of Io's surface and atmosphere and their
 108 interactions with the broader Jovian space environment.

109 **1.2 Spacecraft Exploration of the Galilean Satellites**

110 The most significant advances in our understanding of the Galilean satellites were provided by
 111 spacecraft exploration of the Jupiter system, summarised in Table 2. The *Pioneer 10* and *Pioneer*
 112 *11* flybys provided the first *in-situ* measurements of the Jovian environment and represented the
 113 first spacecraft to be sent to the outer Solar System. These spacecraft obtained the first close-
 114 up images of the Galilean moons, improved diameter measurements of Europa and Callisto, and
 115 improved mass estimates for all four satellites (see Anderson *et al.* 1974; Smith 1978; Morrison
 116 1982), along with the detection of Io's atmosphere and observations of its interaction with the
 117 Jovian magnetosphere. *Pioneer 10* observations also provided confirmation of ground-based ob-
 118 servations (e.g., Kupo *et al.* 1976) of the Io plasma torus, a ring-shaped cloud of electrons and
 119 ionized sulfur and oxygen atoms coincidental with Io's orbit (Frank *et al.* 1976; Intriligator &
 120 Miller 1981).

Mission	Launch Date	Encounter
<i>Pioneer 10</i>	1972 Mar 3	1973 Dec 3; flyby ($1.9 R_{\text{Jup}}$)
<i>Pioneer 11</i>	1973 Apr 6	1974 Dec 3; flyby ($0.6 R_{\text{Jup}}$)
<i>Voyager 1</i>	1977 Sep 5	1979 Mar 5; flyby ($5.0 R_{\text{Jup}}$)
<i>Voyager 2</i>	1977 Aug 20	1979 Jul 9; flyby ($10.4 R_{\text{Jup}}$)
<i>Galileo</i>	1989 Oct 18	1995 Dec 7 - 2003 Sep 21; orbiter
<i>Cassini</i>	1997 Oct 5	2000 Dec 30; flyby ($142.4 R_{\text{Jup}}$)
<i>New Horizons</i>	2006 Jan 19	2007 Feb 28; flyby ($33.2 R_{\text{Jup}}$)
<i>Juno</i>	2011 Aug 5	2016 Jul 5 - present; orbiter

Table 2: Spacecraft Missions to the Jupiter System. Flyby distance to Jupiter expressed in Jupiter radii (1 $R_J = 69173$ km).

121 The *Voyager* encounters in 1979 would reveal the Galilean satellites as four unique and geo-

logically active worlds. The most dramatic discovery of the *Voyager 1* flyby of Io (with a closest approach of just over 20,000 km) was the observation of active volcanic eruption plumes on Io (Morabito *et al.* 1979; Strom *et al.* 1979; Smith *et al.* 1979b). Just prior to the *Voyager 1* encounter, Peale *et al.* (1979) had predicted probable surface evidence of interior melting caused by tidal dissipation of the 4:2:1 Laplacian resonance. Together, the *Voyager* spacecraft also obtained nearly global photographic coverage (see Figure 2) of each satellite (although at varying resolutions), significantly expanding our view of the diverse geological processes shaping their surfaces.



Figure 2: Images of the four Galilean satellites of Jupiter taken by *Voyager 1* during its approach in March 1979. From left to right: Io, Europa, Ganymede, Callisto, shown at their relative sizes. Image credit: NASA/JPL.

More recently, the *Galileo* spacecraft completed a 7-year tour of the Jovian system, completing 34 orbits of Jupiter and several flybys of each moon. Despite limitations to the *Galileo* data stream caused by deployment failure of its high-gain antenna, the larger suite of instrumentation and higher resolution imaging by the *Galileo* spacecraft would provide significant advances in our understanding of the the Galilean satellites. These include new insights into the nature of volcanism on Io and the properties of its crust, the possibility of subsurface liquid water layers on Europa, Ganymede and Callisto, additional measurements of surface and atmospheric compositions, a magnetic field on Ganymede, the interactions between Io's extended atmosphere with Jupiter's magnetosphere and surrounding environment, and improved constraints on interior structures. Along with ongoing ground- and space-based observations (including observations by the *Hubble Space Telescope* and high-resolution imaging by the *Juno* orbiter) the *Voyager* and *Galileo* projects continue to provide the basis of our contemporary scientific understanding of the Galilean worlds. Based upon our current understanding, a summary of the physical properties of the Galilean satellites is given in Table 3, and the inferred interior structures of the Galilean satellites are shown

Parameter	Io	Europa	Ganymede	Callisto
semimajor axis (km)	421800	671100	1070400	1882700
semimajor axis (R_{Jup})	5.90	9.39	14.97	26.33
orbital period (day)	1.769138	3.551181	7.154553	16.689017
radius (km)	1821.6 ± 0.5 [A01a]	1560.8 ± 0.3 [N07]	2634.1 ± 0.3 [D98]	2410.3 ± 1.5 [A01b]
mass (10^{23} kg)	0.89319 ± 0.00012 [A96b]	0.479982 ± 0.000062 [A98]	1.48167 ± 0.0002 [A96a]	1.0759 ± 0.0014 [A01b]
radius (R_M)	1.05	0.90	1.52	1.39
mass (M_M)	1.23	0.66	2.04	1.48
mean density (kg km^{-3})	3528±3	3014±2	1936±1	1834±4
surface gravity (m s^{-2})	1.797	1.315	1.425	1.236
moment of inertia C/MR^2	0.37685 ± 0.00035 [A01a]	$0.3460 (\pm 0.005)$ [A98]	0.3105 ± 0.0028 [A96a]	0.3549 ± 0.0042 [A01b]
geometric albedo [M77]	0.63	0.64	0.43	0.17
ambient Jovian magnetic field (nT) [N98]	1835	420	120	35
magnetic field strength (nT; * = induced)	1300* [K96b]	100-500* [K00,Z00]	719 [K02]	10-50* [K98]

Table 3: Physical Properties of the Galilean Satellites. Sources: [A96a] Anderson *et al.* (1996a); [A96b] Anderson *et al.* (1996b); [A98] Anderson *et al.* (1998); [A01a] Anderson *et al.* (2001a); [A01b] Anderson *et al.* (2001b); [D98] Davies *et al.* (1998); [K96b] Kivelson *et al.* (1996b); [K98] Khurana *et al.* (1998); [K00] Kivelson *et al.* (2000); [K02] Kivelson *et al.* (2002); [M77] Morrison *et al.* (1977); [N98] Neubauer (1998); [N07] Nimmo *et al.* (2007); [Z00] Zimmer *et al.* (2000). Note: 1 R_M = 1 lunar radius = 1737 km ; 1 M_M = 1 lunar mass = 7.25×10^{22} kg; $G = 6.6734 \times 10^{-11} \text{ m}^3 \text{ kg}^{-1} \text{ s}^{-2}$; mean density and surface gravity derived from mass and radius values for each satellite. Cf. Morrison (1982); Lodders & Fegley (1998); Showman & Malhotra (1999); Schubert *et al.* (2004).

in Figure 3. Future proposed and planned missions include two missions designed to study the Galilean moons directly: NASA’s *Europa Clipper* (launched in 2024 and arriving in 2030) and ESA’s *JUICE (JUpiter ICy Moons Explorer)* (launched in 2023 and arriving 2031). Both missions will explore key relationships between satellite subsurfaces, surfaces, and the surrounding Jovian environment, and assess the chemical and biological potential of the subsurface ocean layers.

1.3 Io

1.3.1 Surface features and internal structure

Io is the most volcanically active object in the solar system, with a colorful, sulfur-coated surface dominated by lava flows and dotted with calderas (including saucer-like depressions known as *patera*), along with active volcanic plumes erupting as high as 400 km above the surface (Lopes-Gautier *et al.* 1999; Geissler *et al.* 2004). Imagery from the *Voyager* and *Galileo* missions revealed more than 400 volcanoes on Io, including thermal activity observed at over 150 of them by the *Galileo* NIMS instrument (Lopes *et al.* 2004). In general, volcanic eruption styles have been divided into three major groups: *promethean* eruptions (named after Prometheus volcano), which are characterized by long-lived and extensive lava flows; more violent *pillanian* eruptions (named after Pillan Patera) characterized by rapid outbursts including large plumes and rapid lava flows;

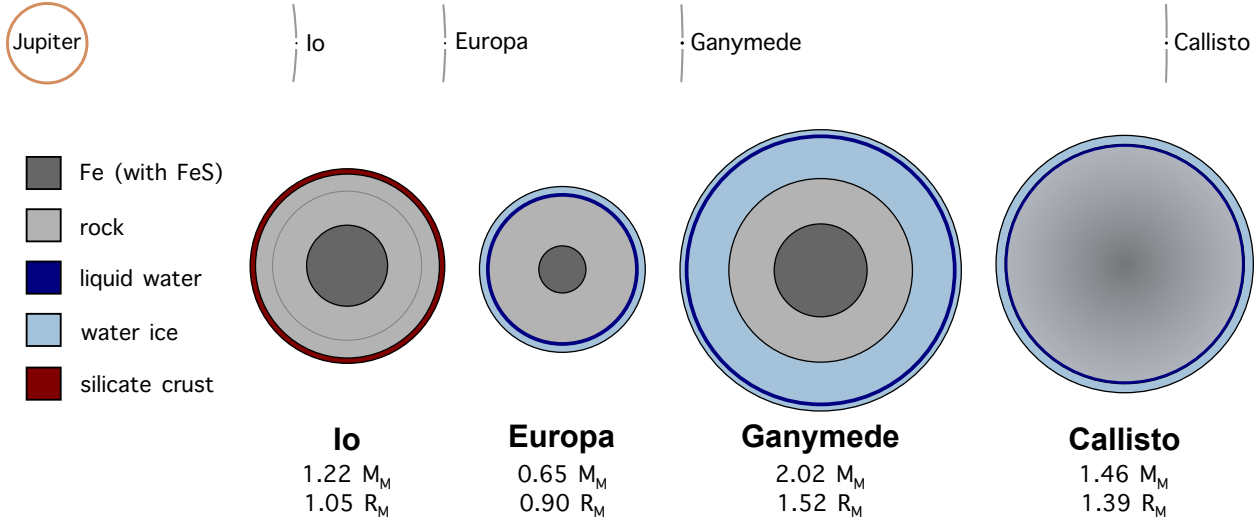


Figure 3: *Top*: Orbital configuration (to scale) and *bottom*: the relative sizes and inferred interior structures of the Galilean satellites. Models and observations indicate differentiated structures for Io, Europa, and Ganymede, and are consistent with the presence of subsurface liquid water layers on Europa, Ganymede, and Callisto. Updated figure adapted after Cruikshank & Morrison (1976).

and *lokian* eruptions (named after Loki Patera) associated with patera and lava lakes. (e.g., see Keszthelyi *et al.* 2001; Lopes-Gautier *et al.* 1999; Lopes *et al.* 2004; Lopes & Spencer 2007). Moreover, Io is nearly devoid of impact craters (Smith *et al.* 1979b), suggesting a very young surface that is continuously resurfaced by ongoing volcanic activity. A few new plumes appear each year, and surface changes are evident over timescales of months, such as the differences observed between the *Voyager 1* and *Voyager 2* encounters in March and July 1977 (respectively), over the course of the *Galileo* mission, and between *Galileo* the *New Horizons* and *Juno* encounters (e.g., Smith *et al.* 1979a; Strom & Schneider 1982; Belton *et al.* 1996), and even between *Juno* orbits (which average 45 days).

The energy driving Io's volcanism is attributed to intense tidal heating, as in the Peale *et al.* (1979) prediction of widespread volcanism at Io prior to the *Voyager 1* encounter. Io orbits Jupiter synchronously at just $5.9 R_{\text{Jup}}$ (roughly similar to the Earth-Moon orbital distance) and is part of the 4:2:1 orbital resonance with Europa and Ganymede. Because the dissipation of orbital energy provides a source of internal heat, the evolution of Laplacian resonance is closely coupled to the thermal and geological history of all three moons (e.g., see Yoder 1979; Lieske 1987; Greenberg 1982; Fischer & Spohn 1990; Malhotra 1991; Showman & Malhotra 1997; Hussmann & Spohn 2004). These gravitational interactions make Io the most tidally deformed and tidally heated satel-

¹⁷⁶ lite in the solar system (e.g., Ojakangas & Stevenson 1986; Segatz *et al.* 1988; Fischer & Spohn
¹⁷⁷ 1990; Matsuyama *et al.* 2022). Infrared observations suggest a global heat flow – typically domi-
¹⁷⁸ nated by a handful of active volcanic regions – on the order of 10^{14} W (Veeder *et al.* 1994; Blaney
¹⁷⁹ *et al.* 1995), suggesting that heating by tidal dissipation is $200\times$ greater than that expected by
¹⁸⁰ radiogenic production (Showman & Malhotra 1999).

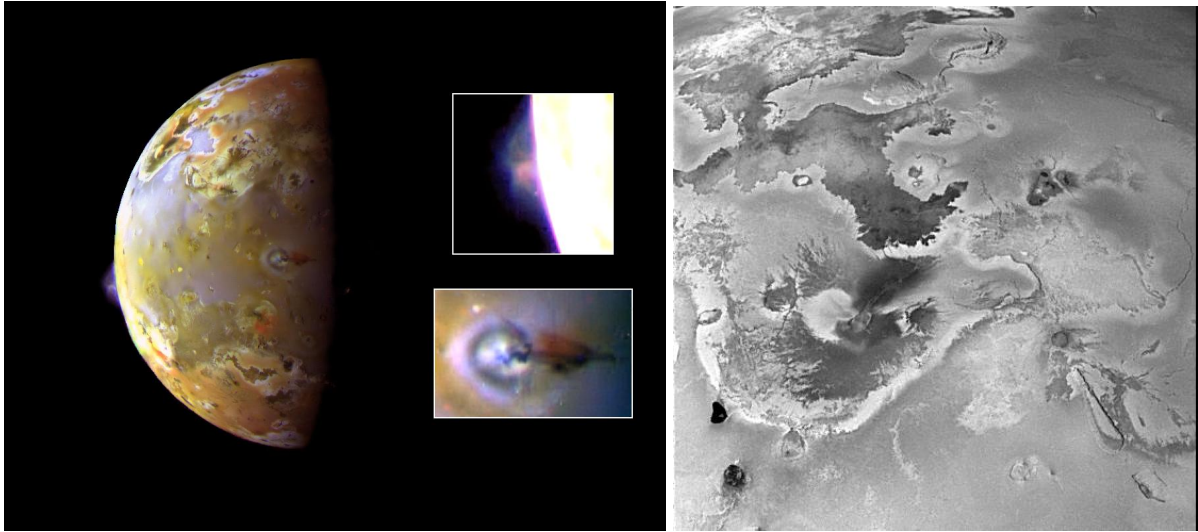


Figure 4: Volcanic features on Io. *Left:* This color image shows two volcanic plumes on Io. One nearly 140-km high plume was captured on the bright limb or edge of the moon (see inset at upper right), erupting over a caldera named Pillan Patera. The second plume, seen near the terminator, is called Prometheus (see inset at lower right). The shadow of the 75-km plume can be seen extending to the right of the eruption vent. The vent is near the center of the bright and dark rings. Plumes on Io have a blue color, so the plume shadow is reddish. Image credit: NASA/JPL, PIA00703. *Right:* A high-resolution *Galileo* image of Io showing immense lava flows and other volcanic landforms. Several high-temperature volcanic hot spots have been detected in this region, consistent with active silicate volcanism in lava flows or lava lakes. The large dark lava flow in the upper left region of the image is more than 400 km long. Image credit: NASA/JPL/University of Arizona, PIA00537.

¹⁸¹ The extent of tidal heating and active volcanic activity has significant implications for Io's in-
¹⁸² ternal structure and suggests a deformable and differentiated interior. Observations of Io's gravity
¹⁸³ field during a close flybys with the *Galileo* spacecraft provided a moment of inertia measurement
¹⁸⁴ (C/MR^2) of 0.378, suggesting a dense central core (Schubert *et al.* 2004), likely consisting of
¹⁸⁵ molten Fe-FeS with a radius ranging from 35–50% of Io's radius (Anderson *et al.* 2001a; Breuer
¹⁸⁶ *et al.* 2022) and overlain by a silicate mantle and lithosphere. However, further structural details re-
¹⁸⁷ main a matter of debate, depending upon the relative extent of magnetic induction, the distribution
¹⁸⁸ and intensity of volcanism, and the extent and location of melting in Io's interior (e.g., see Breuer

¹⁸⁹ *et al.* 2022, for a comparison of Io interior models). For example, a dynamo generated by a molten
¹⁹⁰ Fe-FeS core could possibly generate an intrinsic magnetic field. However, the *Galileo* magne-
¹⁹¹ tometer measurements were ambiguous due to complex interactions with Jupiter’s magnetosphere,
¹⁹² and suggest an induced global magnetic field generated by a strongly conductive layer, such as a
¹⁹³ subsurface silicate melt layer \sim 50 km below the surface (Kivelson *et al.* 1996b, 2001; Khurana
¹⁹⁴ *et al.* 2011), although the measured perturbations may also be caused by interactions between Io’s
¹⁹⁵ plasma torus and atmosphere (Blöcker *et al.* 2018; Šebek *et al.* 2019; Breuer *et al.* 2022). Nu-
¹⁹⁶ merous high mountains on Io – with heights as high as 17.5 km (Boösaule Montes) – suggest the
¹⁹⁷ presence of a relatively thick ($>$ 30 km) lithosphere (Schenk & Bulmer 1998; Schenk *et al.* 2001;
¹⁹⁸ Carr *et al.* 1998b). Although not necessarily volcanic (most volcanic vents on Io are found at low
¹⁹⁹ elevation), Ionian mountains are often found in proximity to volcanic centers, suggesting a causal
²⁰⁰ link, with mountain formation possibly driven by compressive tectonic caused by down-welling
²⁰¹ of older surface material (Schenk & Bulmer 1998; Schenk *et al.* 2001). The mechanical strength
²⁰² required for the extremely high relief of Io’s mountains also suggests a composition of silicate rock
²⁰³ instead of sulfur (Clow & Carr 1980), and provides further evidence for the volcanic and tectonic
²⁰⁴ properties of Io’s crustal materials.

²⁰⁵ 1.3.2 Volcanism and atmospheric chemistry

²⁰⁶ An outstanding question following the *Voyager* encounter was whether Io’s landscape could be
²⁰⁷ best explained by sulfur volcanism or silicate volcanism (e.g., see Carr 1986; Lopes 2007; Johnson
²⁰⁸ 2014). The ubiquitous presence of sulfur-bearing compounds (especially as SO₂) in Io’s spectra,
²⁰⁹ Io’s intense coloration and the presence of colored deposits surrounding volcanic centers (consis-
²¹⁰ tent with varying allotropes of elemental sulfur; e.g. Sill & Clark 1982), and the relatively low
²¹¹ temperatures ($<$ 650 K; Pearl & Sinton 1982) first detected by *Voyager* observations suggested
²¹² the possibility of sulfur volcanism emerging from a sulfur-rich layer either heated from below by
²¹³ silicate magmas (e.g., Sagan 1979) or melted by silicate magma intrusions that yield secondary
²¹⁴ sulfur flows (e.g., Greeley *et al.* 1984). However, subsequent ground-based infrared observations
²¹⁵ indicated magma temperatures much higher than the boiling point of sulfur, suggesting active sil-
²¹⁶ icate volcanism (Johnson *et al.* 1988). Widespread silicate volcanism was confirmed by *Galileo*
²¹⁷ Near-Infrared Mapping Spectrometer (NIMS) observations, revealing a number of volcanic sites

218 with very high temperatures (as high as 2000 K), and spectral and albedo features suggestive of
219 mafic compositions (McEwen *et al.* 1998; Geissler *et al.* 1999). The *Galileo* observations thus
220 suggested that Io's volcanic activity is dominated by silicate volcanism, with deposits of SO₂, S,
221 and silicate pyroclastics mixed within the upper (likely mafic) silicate crust (e.g., Davies 2007).
222 The sulfur deposits in turn provide surface material that may be readily heated and mobilized by
223 silicate magmatism.

224 Io's volcanism and surface materials support a thin (up to \sim 10 nanobar) atmosphere dominated
225 by SO₂ vapor, first detected by the *Voyager 1* IRIS (infrared interferometer spectrometer) in 1979
226 near the Loki volcano (Pearl *et al.* 1979). However, its atmospheric density varies significantly with
227 time and location, depending on local surface properties, insolation, and volcanic activity (e.g.,
228 Spencer & Schneider 1996). For example, higher atmospheric densities have been found on the
229 hemisphere facing away from Jupiter (Jessup & Spencer 2015), regions closer to the equator (such
230 as regions associated with volcanic hot spots), and in the trailing hemisphere. Moreover, ground-
231 based observations have shown the collapse of atmospheric pressure during eclipse as Io enters
232 Jupiter's shadow (Tsang *et al.* 2016), suggestive of condensation of atmospheric SO₂ vapor onto
233 the cooling surface. Thus, although volcanic activity is the ultimate source of the Io atmosphere,
234 the temperature-dependent sublimation of SO₂ ice appears to play a significant role in supporting
235 dayside atmospheric pressures.

236 Several additional species have been detected in the atmosphere of Io, including SO, S, S₂, O,
237 NaCl, and KCl. These are produced by volcanic emission along with subsequent photochemical
238 reactions. For example, UV-driven photolysis of SO₂ (via reactions such as SO₂ $\xrightarrow{\text{h}\nu}$ SO + O and
239 SO₂ $\xrightarrow{\text{h}\nu}$ S + O₂) represents the primary loss process for SO₂ and the main source of atomic oxygen
240 (Kumar & Hunten 1982; Moses *et al.* 2002b,a). The volcanic emission of NaCl, KCl, and S₂ and
241 their subsequent gas-phase chemistry in Pele-type eruptions may yield important clues about the
242 relative contributions of different sources to the atmosphere and into the nature of magma melt
243 composition and equilibria (e.g., McEwen *et al.* 1998; Fegley & Zolotov 2000; Zolotov & Fegley
244 2000; Moses *et al.* 2002b).

245 The escape of neutral atomic species including O, S, Na, and K from Io's atmosphere form
246 an extended cloud that accompanies Io along its orbit. This was first detected by ground-based
247 observations via resonant scattering of sunlight by sodium atoms (Brown & Chaffee 1974). The

248 subsequent escape and ionization of atoms from the extended neutral cloud are trapped by Jupiter's
249 magnetosphere into a co-rotating plasma torus around Jupiter (first discovered via the detection of
250 S+ (Kupo *et al.* 1976)) extending from 5-10 R_J . The high loss rate from the neutral cloud (Spencer
251 & Schneider 1996) and the composition of the torus (dominated by O and S ions) suggest that Io is
252 the primary source for the plasma torus. The composition and chemistry of volcanic processes on
253 Io thus play a central and dynamic role in shaping conditions of the near-Jupiter environment (e.g.,
254 Goertz 1980; Bagal 1994; Spencer & Schneider 1996; Crary *et al.* 1998; Delamere & Bagal
255 2003), including environmental conditions at the surfaces of the other Galilean satellites.

256 1.4 Europa

257 1.4.1 *Interior structure and subsurface ocean*

258 The smallest of the Galilean satellites, Europa has a surface dominated by water ice, the presence
259 of which was first proposed by Kuiper (1957) and Moroz (1961) and later confirmed by ground-
260 based spectroscopic observations (e.g., see Figure 1). This surface ice represents the outermost
261 portion of a shell of water ice up to ~ 100 km thick (e.g., see Anderson *et al.* 1998; Schubert *et al.*
262 2004; Greeley *et al.* 2004). Beneath this shell, the mean density of Europa (3014 kg m^{-3}) implies
263 an interior predominantly composed of silicate rock. Moreover, *Galileo* flyby measurements of
264 Europa's moment of inertia give $C/MR^2 \approx 0.35$ (Anderson *et al.* 1997a, 1998), suggesting
265 a differentiated interior. Using constraints provided by the gravity data and plausible chemical
266 compositions, most interior structure models include three main layers: a metallic (Fe and Fe-
267 FeS) core, a silicate mantle, and an outer shell of H₂O ice (see Figure 3; Schubert *et al.* 2004;
268 Showman & Malhotra 1999), with variations in model thickness estimates due to different density
269 assumptions for each interior layer. An analysis of impact crater morphology demonstrated an
270 outer ice shell thickness of at least several km but possible excavation by large craters – which show
271 enhanced viscous relaxation – to warm ice or even liquid water suggest an outer shell thickness
272 of ~ 20 km (Moore *et al.* 1998, 2001; Schenk 2002). The arrangement of surface features also
273 provide evidence in support of true polar wander (e.g., Leith & McKinnon 1996; Schenk *et al.*
274 2008) of an outer ice shell decoupled from the interior by the subsurface ocean layer.

275 Indeed, the *Galileo* gravity data along with other surface geologic features observed by *Voyager*

and *Galileo* were strongly suggestive of the presence of a subsurface liquid water layer (Carr *et al.* 1998a; Pappalardo *et al.* 1998b, 1999; Greeley *et al.* 2004). Further compelling evidence was provided by *Galileo* magnetometer measurements, which detected an induced dipole generated by a conductor within Jupiter’s magnetic field (Khurana *et al.* 1998; Kivelson *et al.* 2000; Zimmer *et al.* 2000) – indicative of a conducting layer in Europa’s interior. This behavior is most plausibly consistent with the existence of a salty conducting subsurface ocean at the base of the outer ice layer. Although the estimated thickness of the ocean layer depends on assumptions about the conductivity of the water (a more conductive layer allows for a thinner layer; a terrestrial seawater composition would allow for a layer as thin as 3.5 km; cf. Zimmer *et al.* 2000), and/or its possible distribution as a partial melt within the lower ice shell, the observations are generally consistent with a layer of salty water at least several kilometers thick. Furthermore, thermal models that account for tidal heating – along with observational and chemical constraints – suggest an ice shell a few tens of km thick, with an ocean layer up to \sim 100 km thick (e.g., Spohn & Schubert 2003; Hussmann *et al.* 2002). The presence of a subsurface ocean has profound implications for the potential habitability of the interior, and numerous studies have explored the conditions under which this environment could support life (e.g., see Reynolds *et al.* 1983; Kargel *et al.* 2000; Greeley *et al.* 2004; Glein *et al.* 2015; Journaux *et al.* 2017; Vance *et al.* 2018).

Europa’s interior is heated primarily through tidal dissipation resulting from its participation in the 4:2:1 mean-motion resonance with Io and Ganymede. However, it remains uncertain whether this resonant configuration has persisted throughout Europa’s history, and the thermal evolution of its interior depends on assumptions about the rate of tidal heating, the rheological properties of the ice shell, and the thermal conductivity of the rocky mantle (e.g., Hussmann *et al.* 2002; Hussmann & Spohn 2004). In combination with radiogenic heating, and in the absence of significant antifreezing solutes, tidal dissipation is likely essential in maintaining Europa’s subsurface ocean (Cassen *et al.* 1981). Depending on the dissipation mechanisms, frictional heating and flexing within the ice shell and underlying liquid layer could produce substantial energy, not only sustaining the liquid ocean but potentially driving hydrothermal activity at the seafloor (Tyler 2008; McCarthy & Cooper 2016).

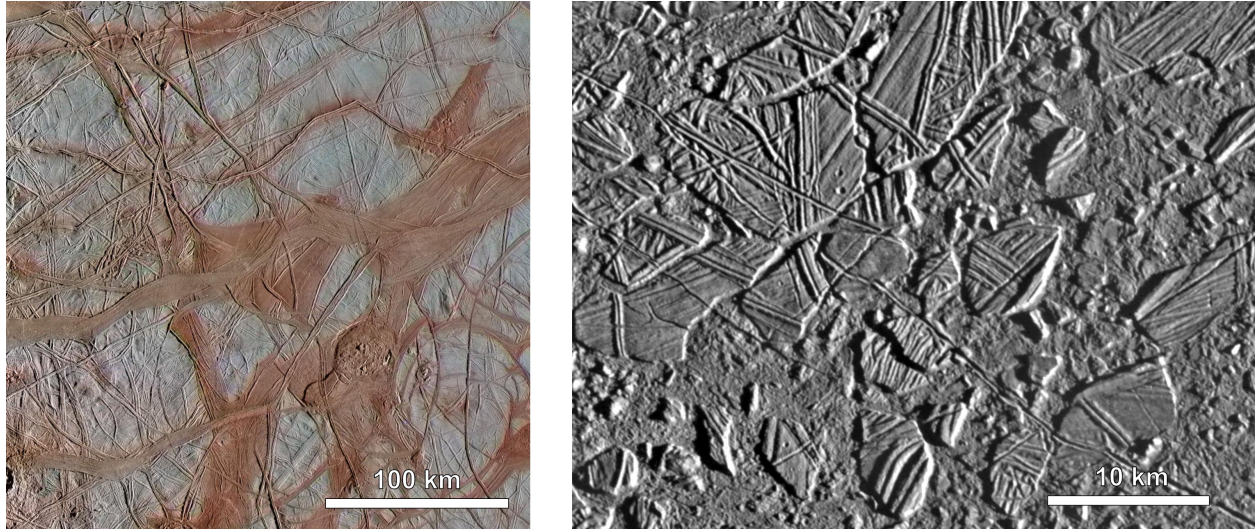


Figure 5: *Galileo* images of representative terrains found on the surface of Europa. *Left*: a region of overlapping bands and ridges, with regions of chaos terrain. Image credit: NASA/JPL-Caltech/SETI Institute, PIA23872. *Right*: a closer view of Conamara Chaos, a region showing disruption of the icy crust into separate blocks. Image credit: NASA/JPL/ASU, PIA00591.

304 1.4.2 Surface geology and chemistry

305 The small number of impact craters on Europa suggests active geology and a relatively young sur-
306 face age (Smith *et al.* 1979a; Lucchitta & Soderblom 1982; Figueredo & Greeley 2004) estimated
307 to be on the order of $10^7 - 10^8$ yr (Greeley *et al.* 2004; Zahnle *et al.* 1998), implying that Europa's
308 outer shell is being actively reworked (although no significant changes were observed between the
309 *Voyager* and *Galileo* missions). The moon's surface morphology points to widespread tectonic
310 activity, possibly involving the movement and deformation of ice along fractures, along with dis-
311 rupted regions that suggest that internal processes – such as convective overturn or tidal heating –
312 may locally warm the ice shell. This heating could result in partial melting near the base of the
313 crust, promoting the ascent of warm ice or even cyrovolcanism. Together, these features show that
314 Europa's tidal heating and interior structure play a key role in shaping its surface geology.

315 Following the classification of Lucchitta & Soderblom (1982) based on *Voyager* imaging, the
316 exceptionally smooth icy surface has traditionally been divided into two basic regions of smooth
317 plains and mottled terrain. Both units are frequently transected by long light and dark lineaments of
318 bands and ridges which cover most of the surface. Although the formation of bands are generally
319 attributed to crustal extension as an icy analog to terrestrial mid-ocean ridges (e.g., Prockter *et al.*

320 2002), a number of different models have been proposed to explain the formation of Europa's
321 ubiquitous ridges. As summarized by the review in Greeley *et al.* (2004), these include tidal
322 squeezing, linear volcanism, dike intrusion, compression, linear diapirism, shear heating, or triple
323 banding from cryovolcanism. A commonality of these models is the role of warmer ductile ice
324 or possibly liquid water, further demonstrating key relationships between the interior structure of
325 Europa's water-ice shell and its surface morphology. Among the mottled regions are found *chaos*
326 terrains of disrupted crustal blocks evocative of rafting of polar sea ice on Earth (see Figure 5)
327 and *lenticulae* of roughly circular domes or pits ~ 10 km in diameter. A proposed formation
328 mechanism for these regions is the diapiric upwelling of relatively warm buoyant ice or possibly
329 liquid water, leading to disruption or partial melting of outer ice layers (e.g., Carr *et al.* 1998a;
330 Pappalardo *et al.* 1998b; Rathbun *et al.* 1998; Collins *et al.* 2000).

331 Although the surface of Europa is predominantly fine-grained water ice, darker regions – gener-
332 ally associated with ridges and chaos regions and the more reddish trailing hemisphere – indicate
333 the widespread presence of non-ice component(s) (e.g., Pollack *et al.* 1978; Calvin *et al.* 1995;
334 Carlson *et al.* 2009). The large deviations in the *Galileo* NIMS absorption features of water ice in
335 these regions suggest hydrated minerals – first proposed by Clark (1980) by comparison of labo-
336 ratory spectra with ground-based infrared reflectance spectra from Clark & McCord (1980) – such
337 as magnesium sulfate hydrate ($MgSO_4 \cdot nH_2O$) with some sodium sulfate hydrate ($Na_2SO_4 \cdot H_2O$)
338 (McCord *et al.* 1998, 1999, 2001), or possibly hydrated sulfuric acid ($H_2SO_4 \cdot nH_2O$) (Carlson *et al.*
339 1999b, 2009). These materials are colorless, but would be subject to irradiation that would darken
340 and redden their color via the formation of polymeric sulfur allotropes (S_n) (Greeley *et al.* 1998;
341 Johnson *et al.* 1983; Spencer *et al.* 1995; Nelson *et al.* 1986). Moreover, the spectral uniformity of
342 these materials suggests a well-mixed source region, possibly derived from the subsurface ocean
343 layer as brine, and/or the exogenic delivery of sulfur-rich material from Io (Showman & Malhotra
344 1999; Carlson *et al.* 1999b, 2009). However, the observed correlation of putative hydrates with
345 geologic features (McCord *et al.* 1998, 1999; Fanale *et al.* 2000) and with the distribution of de-
346 tected SO_2 (Noll *et al.* 1995; Domingue & Lane 1998; Hendrix *et al.* 2011) suggests at least some
347 endogenic (i.e., subsurface ocean) association. The recombination of H_2O ice and SO_2 frost could
348 also react to form sulfuric acid, completing a radiolytic sulfur cycle, $S \rightarrow H_2SO_4 \rightarrow SO_2 \rightarrow S$ (Carl-
349 son *et al.* 1999b), with inputs from either endogenic sulfate salts or exogenic implantation. Other

detected species include the detection of H₂O₂ by infrared absorption (Carlson *et al.* 1999a), likely a radiolytic product from a water ice source and an identified ultraviolet absorber on the trailing side attributed to a sulfur species (Hendrix *et al.* 1998). Carbon dioxide (CO₂) has also been detected on Europa (Smythe *et al.* 1998), with a distribution correlated with the dark hydrate regions (Hansen & McCord 2008). This is suggestive of an endogenic source, although the production pathway of CO₂ remains uncertain (Carlson *et al.* 2009).

Europa possesses a tenuous, surface-bounded (i.e. molecular collisions with the surface are more likely than gas-phase collisions) atmosphere primarily generated through radiolysis and sputtering of its icy surface (see Johnson *et al.* 2009; McGrath 2014) within its harsh radiation environment. The atmosphere was first detected by the emission of atomic oxygen formed by the excitation and dissociation of O₂ (Hall *et al.* 1995), and confirmed by *Cassini* UVIS measurements that showed an extended oxygen atmosphere. Oxygen airglow measurements from Hubble Space Telescope (HST) ultraviolet spectra show a column density of 10¹⁴–10¹⁵ cm⁻² (Hall *et al.* 1998) — many orders of magnitude lower than Earth’s atmosphere (10²⁵ cm⁻²). The dominant source of this oxygen is sputtering, caused by the bombardment of Europa’s surface by energetic ions and electrons from Jupiter’s magnetosphere. These high-energy collisions not only liberate water molecules from the ice but also lead to the production of molecular oxygen and hydrogen (H). The lighter hydrogen readily escapes, forming the main component of Europa’s neutral torus (Mauk *et al.* 2003; Roth *et al.* 2017b). Trace elements such as sodium and potassium have also been detected in Europa’s extended atmosphere (Brown1996Natur.380..229B, Brown2001Icar..151..190B). The observed Na/K ratio (~ 20) is higher than that expected for Io-genic (~ 10) or meteoritic (~ 13) sources, suggesting an endogenic source possibly consistent with material derived from the subsurface ocean (Zolotov & Shock 2001; Johnson *et al.* 2009).

More recently, observations by the *Hubble Space Telescope* (HST) detected ultraviolet emissions consistent with localized hydrogen and oxygen, suggesting the presence of transient plumes of water vapor erupting from near Europa’s south pole (Roth *et al.* 2014). Supporting this, a re-analysis of magnetometer and plasma wave data from *Galileo*’s closest flyby of Europa in 1999 revealed magnetic field disturbances and plasma signatures consistent with the spacecraft having passed through an active plume (Jia *et al.* 2018). However, these detections are often near instrument sensitivity limits, indicating that that plumes on Europa are relatively small (< 30 km)

and episodic, with eruptions more likely to occur near points of maximum tidal stresses during Europa’s orbit (Roth *et al.* 2014; Quick *et al.* 2013; Paganini *et al.* 2020; Jia *et al.* 2021). In any case, the existence of plumes points to a clear endogenous origin—possibly driven by tidal flexing and cryovolcanism—originating either from the subsurface ocean or from water reservoirs within the ice shell. The plumes may therefore offer a unique opportunity to sample the chemistry, and potentially even biosignatures, of Europa’s subsurface water without the need to land or drill. This possibility is a key scientific objective of NASA’s Europa Clipper mission, launched in 2024 and expected to reach Jupiter’s system in 2030 (e.g., see Pappalardo *et al.* 2024).

1.5 Ganymede

1.5.1 Interior structure and surface geology

Ganymede is the largest satellite in the Solar System, with a diameter that exceeds that of both Mercury and Pluto. As noted above, *Pioneer* observations allowed for accurate measurements of density, revealing – along with Callisto – a lower density suggestive of bulk composition of rock and ice. Following the *Voyager* encounters, an ongoing question was the extent to which Ganymede’s interior of mostly rock and ice was differentiated (e.g., Cassen *et al.* 1981). Analysis gravity field measurements from *Galileo* flybys strongly suggested that Ganymede is highly differentiated, with a moment of inertia (C/MR^2) of 0.3105 (Anderson *et al.* 1996a; Schubert *et al.* 2004) – the lowest measured value of any solid body in the Solar System (Showman & Malhotra 1999). Notably, *Galileo* magnetometer measurements also revealed the presence of an intrinsic magnetic field (Kivelson *et al.* 1996a, 2000), with a surface field strength several times stronger than the ambient Jovian field present at Ganymede’s orbit. The presence of a magnetic field and interior models are consistent with the presence of a dynamo generated in a liquid Fe-FeS core (Anderson *et al.* 1996a; Schubert *et al.* 1996; Schubert *et al.* 2004), which would require the persistence of core convection into the present day (e.g., see Showman & Malhotra 1999). This condition is possibly met by top-down crystallization scenarios of either Fe (“iron snow”) or FeS in the core, both of which could generate the observed field at Ganymede (Rückriemen *et al.* 2018). Other authors have proposed that the source of the present magnetic field is remanent magnetization from an earlier, stronger field (e.g., Crary & Bagenal 1998).

408 Data acquired by the *Galileo* magnetometer over a series of flybys also indicated deviations
 409 in Ganymede's magnetic dipole, suggestive of a conductive layer in Ganymede's outer layers,
 410 consistent with the presence of a thin (on the order of tens of km) subsurface liquid water ocean
 411 (Kivelson *et al.* 2002). A comparison of an inferred thermal profile of Ganymede and the ice
 412 phase diagram (see Figure 6) suggests that the ocean layer may be formed by melting at \sim 170
 413 km depth below Ganymede's surface – near the minimum in the water ice liquidus at the Ice-I
 414 and Ice-III phase transition – or possibly shallower depending upon the presence sulfates, halide
 415 salts, or ammonia (e.g., Kivelson *et al.* 2002; Pappalardo *et al.* 2004; Spohn & Schubert 2003).
 416 Internal structure models (see Figure 3) thus typically include an Fe-FeS core and rocky mantle,
 417 surrounded by a thick outer layer of mostly water ice with an intervening subsurface liquid layer.
 418 The actual thickness of the ocean layer depends upon several factors including the extent of tidal
 419 heating, thermal conductivity, and ocean composition. For example, thermal models show that the
 420 presence of even small (\sim 5%) concentrations of NH₃ would further reduce the triple point and
 421 could allow for a thicker oceans (up to 230 km on Ganymede; see Spohn & Schubert 2003).

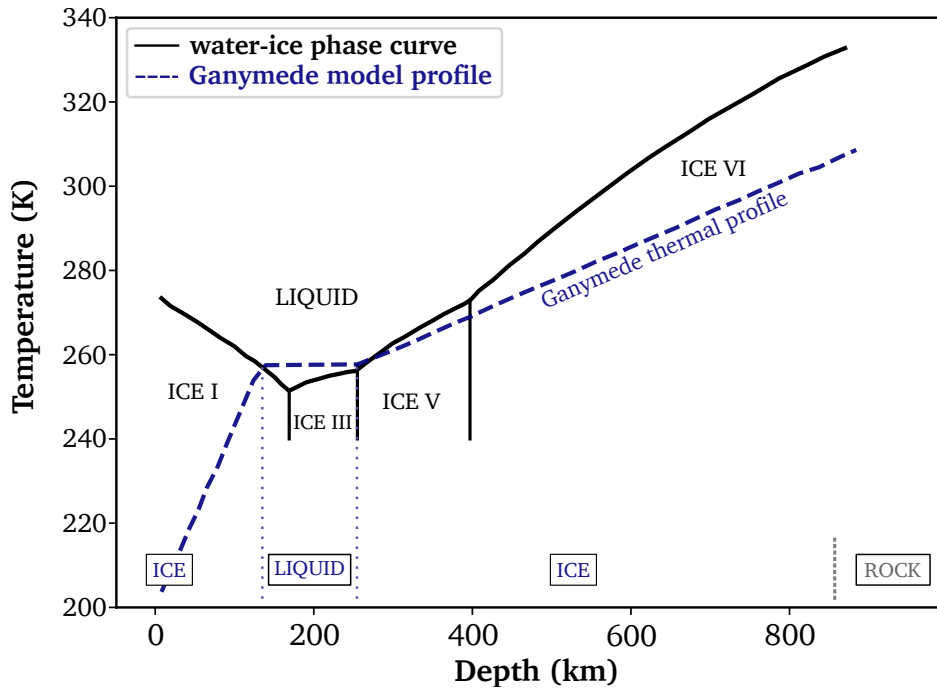


Figure 6: A comparison of the phase diagram of water ice (black line) and a speculative thermal profile of Ganymede (dashed blue line). The ocean layer may be located near the minimum in the melting temperature of ice near the Ice-I and Ice-III phase transition, or wherever the thermal profile is warmer than the liquidus curve. The bottom labels indicate the phase expected in Ganymede's interior as a function of depth. After Cassen *et al.* (1981) and Kivelson *et al.* (2002).

422 Although Ganymede and Callisto are roughly similar in size and density, the highly differenti-
423 ated structure of Ganymede implies significantly greater interior heating, attributed to its participa-
424 tion in the 4:2:1 Laplacian resonance with Io and Europa. Tidal heating from this orbital resonance
425 also appears to be responsible for Ganymede's relatively active surface geology, shaped by impact
426 cratering, cryovolcanism, and widespread tectonic deformation. The surface of Ganymede is gen-
427 erally divided into two primary types of terrain: *dark terrain* and *bright terrain* (e.g., Shoemaker
428 *et al.* 1982; Pappalardo *et al.* 2004). The *dark terrain* covers about one-third of the surface and
429 is more heavily cratered, implying an ancient surface age (e.g., see Zahnle *et al.* 1998, 2003). A
430 common feature of dark terrain are large systems of furrows, up linear and curvilinear grooves up
431 to ~ 100 km in length and bounded by raised ridges. The furrows are believed to have formed
432 during basin collapse associated with large multi-ring structures around major impact basins, with
433 present-day furrows representing remnants of these systems mostly erased by later tectonic activity
434 (McKinnon & Melosh 1980). The *bright terrain* on Ganymede (see Figure 8) covers about two-
435 thirds of the surface and consists of grooves (commonly 10s of km in width) that transect the dark
436 terrain and intersect and overlap one another. In addition to their stratigraphic relationship, the
437 bright terrain has a much lower crater density than the dark terrain, implying a relatively younger
438 age (Zahnle *et al.* 1998, 2003). Across both terrain types, surface features are consistent with the
439 mechanical properties of ice, and crater morphologies (especially of larger craters) are consistent
440 with the presence of more viscous, warmer ice at depth and/or a subsurface ocean. (e.g., Schenk
441 1991, 2002).

442 The grooved terrains are dominated by extensional tectonic forces. Following *Voyager*, a
443 graben-like formation mechanism was favored, in which extensional rifting would allow the extru-
444 sion of water or warm ice pulled apart – akin to terrestrial seafloor spreading – as the rift pulled
445 apart to form relatively smooth regions and parallel grooves (e.g., see Shoemaker *et al.* 1982). The
446 higher resolution imagery provided by *Galileo* supported the rifting model, but revealed a much
447 greater extent of fractures and fault-bounded ridges suggesting that extensional tectonics plays a
448 larger role than cryovolcanism in bright groove formation (e.g., see Pappalardo *et al.* 1998a, 2004).
449 Models of groove distributions have also suggested that groove formation may be tied to large-scale
450 structure(s) present in Ganymede's lithosphere, possibly including the dark terrain furrows as stru-
451 ctures of pre-existing weakness (e.g., Murchie *et al.* 1986; Collins *et al.* 1998; Pappalardo *et al.*

452 1998a; Showman & Malhotra 1999; Pappalardo *et al.* 2004).

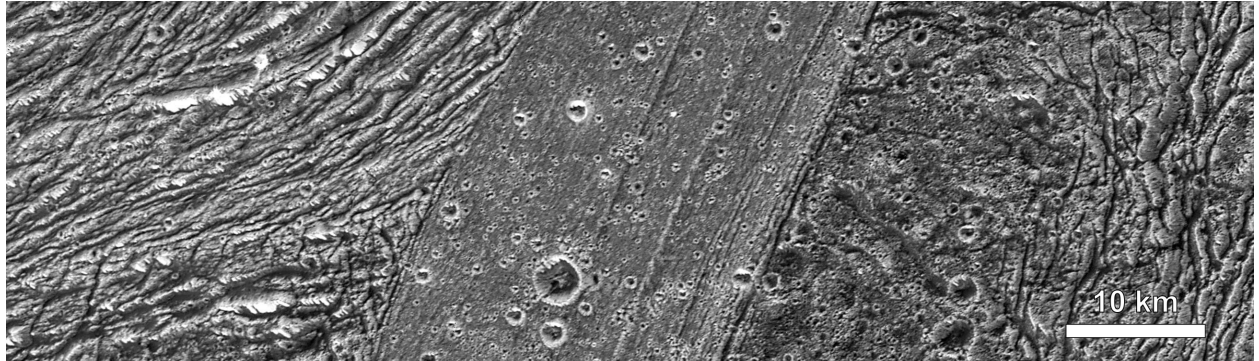


Figure 7: A high-resolution (34 m/pixel) *Galileo* image showing a mix of terrains on Ganymede. The smooth bright Arbela Sulcus is the youngest terrain here, slicing north-south across the image. It is finely striated, and relatively lightly cratered. To the east (right) is the oldest terrain in this area, rolling and relatively densely cratered Nicholson Regio. To the west (left) is a region of highly deformed grooved terrain, intermediate in relative age. In this area of grooved terrain, stretching and normal faulting of Nicholson Regio has deformed it beyond recognition. Image credit: NASA/JPL/Brown University, PIA02572.

453 *1.5.2 Surface composition, atmosphere, and environment*

454 As for Europa, early spectroscopic observations of the surface indicated the widespread presence
455 of water ice, although with a comparatively greater proportion of dark non-ice material (e.g., see
456 reviews in Sill & Clark 1982; Calvin *et al.* 1995; Greeley *et al.* 2004). The surface appearance
457 is interpreted as a relatively thin veneer of low-albedo material (such as silicate-rich material)
458 that overlies a brighter icy substrate, such that exposure of this substrate via impact cratering or
459 tectonic activity produces variations in surface brightness (e.g., Prockter *et al.* 1998). Analysis
460 of the *Galileo* NIMS spectra of Ganymede suggests the presence of hydrated minerals similar
461 to those on Europa. Moreover, the trailing side of Ganymede is darker and appears to contain
462 larger (more crystalline) ice grains than on the leading side, for which the infrared observations
463 suggest a larger proportion of finer-grained water ice. This pattern is consistent with a sputtering
464 process that would remove ice from the trailing side and re-deposit on colder or higher-albedo
465 surfaces elsewhere, such as the poles and/or the leading side (McCord *et al.* 1998, 2001). Although
466 tidal heating on Ganymede is relatively modest today, excitation of Ganymede's eccentricity as it
467 entered the Laplacian resonance may have enhanced tidal heating (Showman & Malhotra 1997;
468 Showman *et al.* 1997; Showman & Malhotra 1999). Thermal models suggest that this increased

469 heating, along with a shallower depth to the liquid layer, may have resulted in the delivery of
470 hydrated salts (such as MgSO₄, Na₂SO₄, or H₂SO₄ hydrates) from a briny subsurface ocean (e.g.,
471 McCord *et al.* 2001).

472 In addition to ice and hydrated minerals, a number of other minor components have been
473 discovered on or near Ganymede's surface. Molecular oxygen (O₂) and ozone (O₃) were detected
474 by telescopic observations (Nelson *et al.* 1987; Noll *et al.* 1996; Spencer *et al.* 1995; Hendrix *et al.*
475 1999) – possibly trapped in voids on the icy surface – with enhanced concentrations on the trailing
476 side. Spectra from Galileo NIMS observations also show absorption features consistent with CO₂,
477 C≡N bonds, and C-H bonds, and SO₂ (McCord *et al.* 1997, 1998). The carbon-bearing species
478 appear to be enhanced in the dark terrain and are possibly produced via charged particle irradiation
479 of carbon- and nitrogen-bearing compounds in the surface ice. The presence of SO₂ may be due to
480 implantation of Io-derived sulfur and/or radiolysis of sulfur present in surface ices. As for Europa,
481 the relative roles of the exogenic vs. endogenic processes shaping spectral properties remains an
482 ongoing question.

483 Ganymede has a tenous atmosphere, first detected by oxygen airglow measurements from *Hub-*
484 *ble Space Telescope (HST)* ultraviolet spectra, indicating an oxygen column density of 10¹⁴-10¹⁵
485 cm⁻², similar to that above Europa (Hall *et al.* 1998) and likewise produced by ion and electron
486 bombardment and of the surface ice. Hydrogen ions have also been detected above Ganymede and
487 in the surrounding space (Barth *et al.* 1997; Frank *et al.* 1997), suggesting a net loss of H₂O from
488 the surface. Taken together, sputtering and sublimation of surfaces ices may lead to preferential
489 deposition of water frost near polar regions and an escape flux equivalent to a few meters of surface
490 per million years (Barth *et al.* 1997; Frank *et al.* 1997), although the formation and presence of a
491 non-ice protective veneer could significantly prolong this process to geologic timescales.

492 1.6 Callisto

493 1.6.1 Interior structure and surface geology

494 The outermost of the Galilean moons, Callisto is roughly the size of Mercury. Early observations
495 of Callisto suggested similarities with its sibling Ganymede, with a density consistent with a bulk
496 composition of rock and ice. The *Voyager* encounters would reveal a surface shaped by impact

497 craters over all scales – from large impact basins down to the \sim 1 km resolution of *Voyager* imaging
498 and lacking large-scale endogenic volcanic or tectonic features (Smith *et al.* 1979b,a). Despite
499 their bulk similarities, the dramatic differences in the surface geologies of Ganymede and Callisto
500 have thus continued to invite comparison and exploration of their different evolutionary paths.

501 Leading up to and following *Voyager*, an ongoing question was whether Callisto’s interior was
502 a primordial differentiated mixture of rock and ice, or at least partially differentiated, with an icy
503 mantle overlying a rockier interior (Schubert *et al.* 1981; McKinnon & Parmentier 1986; Schubert
504 *et al.* 2004). Earlier models of Callisto’s structure and thermal evolution suggested that radiogenic
505 heating could lead to melting and differentiation (Lewis 1971a,b), although solid convection would
506 yield frozen mantle layers (Reynolds & Cassen 1979; Cassen *et al.* 1981). Moreover, Callisto lacks
507 the tidal heating effects of the other Galilean satellites, as it does not participate in the 4:2:1 Lapla-
508 cian resonance. This difference in orbital configuration is generally attributed as a primary factor
509 driving evolutionary differences between Callisto and Ganymede. Gravity measurements from
510 Galileo flybys showed yielded a moment of inertia (C/MR^2) of 0.3579 (Anderson *et al.* 1997b;
511 Schubert *et al.* 2004). This is lower than the value of 0.38 expected for a completely homoge-
512 neous interior (McKinnon 1997), suggesting that Callisto is at least partially differentiated (e.g.,
513 see Nagel *et al.* 2004, for a discussion of subsolidus differentiation). Following *Galileo*, interior
514 models therefore show that the relatively proportion of rock and metal increases with depth (e.g.,
515 see Figure 3), although the precise distribution of these materials in distinct layers or in a gradient
516 cannot be determined from the data (Schubert *et al.* 2004). Studies of Callisto’s surface geology
517 suggests that the outermost \sim 10 km of Callisto may be chemically differentiated, producing an
518 upper ice-rich crust mixed with rocky material (Schenk 1995). Magnetometer measurements from
519 *Galileo* flybys revealed the signature (seen more clearly at Callisto than Ganymede, due to the lat-
520 ter’s intrinsic magnetic field) of a conducting layer in Callisto’s shallow subsurface (Khurana *et al.*
521 1998; Kivelson *et al.* 1999; Zimmer *et al.* 2000), consistent with the presence of a liquid ocean
522 layer \sim 10 km thick assuming water of terrestrial salinity. Melting in Callisto’s subsurface ice to
523 produce the liquid layer may follow a mechanism similar to that proposed for Ganymede (e.g.,
524 see Figure 6 and Cassen *et al.* 1981; Schubert *et al.* 2004). However, maintaining an ocean in the
525 absence of tidal heating is more challenging, and several models have proposed the existence of a
526 compound such as ammonia that may be required to provide sufficient freezing point depression in

527 the liquid layer (e.g., Kargel *et al.* 1991; Kargel 1992; Hogenboom *et al.* 1997; Spohn & Schubert
528 2003).

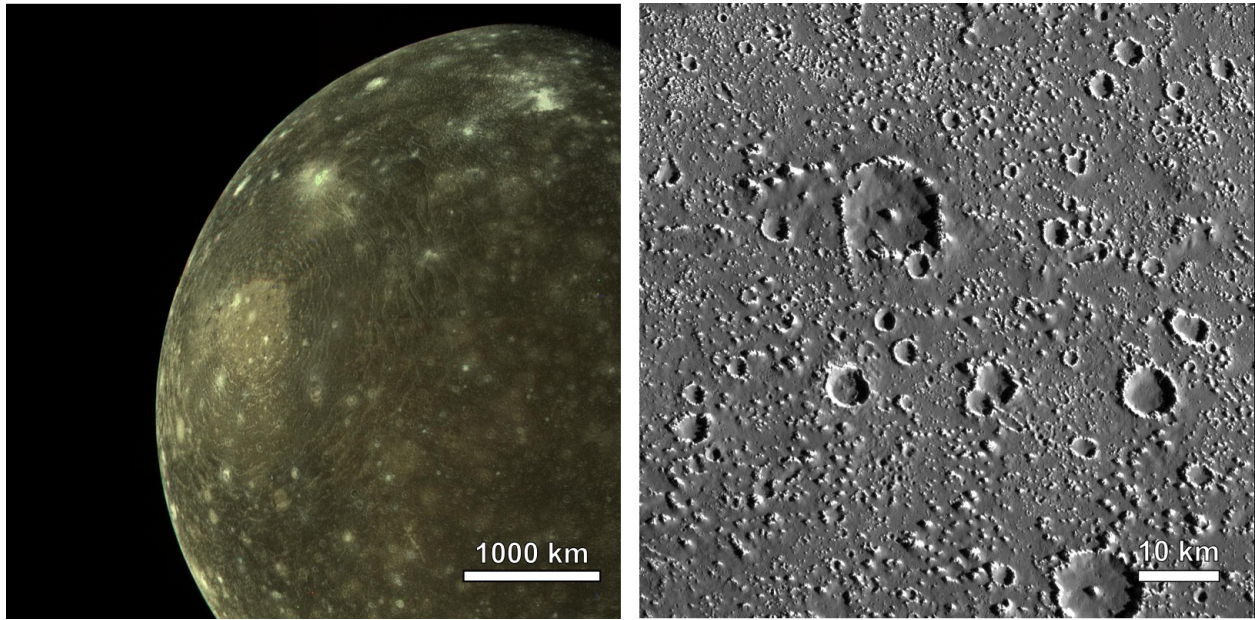


Figure 8: *Left:* Callisto’s Valhalla impact crater imaged by *Voyager 1*, showing a large (~ 600 km) bright central region and vast multi-ring system. (Image credit: NASA/JPL, PIA00080.) *Right:* Higher resolution *Galileo* image of Callisto’s cratered plains showing a smooth dark blanket of material and relatively few of the smallest craters compared to the surface of Ganymede. (Image credit: NASA/JPL, PIA01631.)

529 At all scales imaged by *Voyager* ($\gtrsim 1$ km), the cratered plains of Callisto approach saturation
530 (i.e., the formation of a new impact crater would destroy a previous one), and impact cratering
531 appears to have been the dominant geologic process shaping the surface. Callisto also hosts two
532 very large impact basins, including Valhalla, which – at a 3800 km diameter – is the largest multi-
533 ring impact basin in the Solar System. Unlike lunar impact basins, the bright concentric rings of
534 Valhalla (and its smaller sibling Asgard) have little topographic relief and are consistent with for-
535 mation via failure of a relatively thin outer brittle “lithospheric” layer, followed by inward flow of
536 warmer “asthenospheric” material to replace the impact’s excavation cavity (McKinnon & Melosh
537 1980; Schenk 1995).

538 At the small end of the scale, the higher resolution imagery ($\lesssim 1$ km) from *Galileo* revealed
539 that many of Callisto’s surface features have been subject to intense degradation, and Callisto has
540 a *lower* crater frequency than Ganymede at these sizes (e.g., Greeley *et al.* 2000; Moore *et al.*

541 2004). The erosional loss of small craters appears to be driven by sublimation and disaggregation
542 of “bedrock” surface material, followed by mass movement to the surrounding dark plains units
543 (e.g., Moore *et al.* 1999, 2004). The presence of a more volatile ice such as NH₃ or CO₂ has also
544 been proposed to explain the enhanced rate of degradation on the surface of Callisto (which would
545 have accreted at lower temperatures and thus may have retained more ammonia hydrate or CO₂
546 ice, e.g., see Lunine & Stevenson 1985; Mousis & Alibert 2006) compared to Ganymede (Moore
547 *et al.* 1999). The continuous bombardment by micrometeoroids and energetic ions may also erode
548 and smooth the plains over time. Bright crater rims and ridges among the dark lower-lying plains
549 deposits are consistent with Callisto’s dark surface appearance overall (average albedo of ~0.2),
550 marked by small brighter regions of up to ~0.8 albedo that are often associated with impact craters
551 and basin rings (e.g., see Figure 2) and with topographic highs more generally (such as ridges or
552 crater rims) suggesting the presence of frost at higher elevations (e.g., Lebofsky 1975; Squyres
553 1980; Spencer & Maloney 1984; Greeley *et al.* 2000; Moore *et al.* 2004).

554 1.6.2 *Surface composition, atmosphere, and environment*

555 As for Europa and Ganymede, early telescopic infrared observations of Callisto consistently
556 demonstrated the dominance of water ice absorption features (e.g., Pilcher *et al.* 1972; Clark &
557 McCord 1980; Sill & Clark 1982), although comparison with laboratory spectra suggested that
558 the surface of Callisto contains a relatively larger fraction of non-ice materials (e.g., Roush *et al.*
559 1990; Calvin & Clark 1991; Calvin *et al.* 1995). This was confirmed by Galileo NIMS obser-
560 vations, which suggests a surface generally consisting of 60-80% non-ice components (such as
561 hydrated silicate minerals or possibly carbonaceous material) with patches that are ice-free and
562 patches of nearly pure ice (McCord *et al.* 1997, 1998; Moore *et al.* 2004). The composition of
563 the non-ice component is consistent with hydrated minerals that contain oxidized iron (Fe⁺² and
564 Fe⁺³) and Mg-OH bearing minerals (Calvin & Clark 1991; Moore *et al.* 2004).

565 The *Galileo* NIMS observations (McCord *et al.* 1997, 1998) and more recent JWST observa-
566 tions (e.g., Cartwright *et al.* 2024) of Callisto’s surface showed a 4.25 μm spectral feature identified
567 as CO₂ ice. Because the observed CO₂ feature is inconsistent with either vapor or frost, and be-
568 cause CO₂ would be expected to rapidly sublimate at Callisto daytime surface temperatures (165
569 K), McCord *et al.* (1998) proposed its presence as trapped CO₂ molecules in gas or fluid inclusions

570 within surface materials. The distribution of CO₂ is asymmetric, with higher CO₂ concentrations
571 on the trailing side (McCord *et al.* 1998; Hibbitts *et al.* 2000, 2002). This is suggestive of radiation
572 effects playing in the production of CO₂ or conditions for CO₂ inclusions, although impact fea-
573 tures that show enhanced CO₂ (Hibbitts *et al.* 2002) are suggestive of a primordial source of CO₂.
574 Ultraviolet and infrared observations of Callisto also show features that are consistent with the pres-
575 ence of SO₂ (Noll *et al.* 1997; Lane & Domingue 1997; McCord *et al.* 1998), possibly existing as
576 trapped molecules in the same way as CO₂. Io is a plausible source of sulfur in surface materials
577 throughout the Galilean system; however, the SO₂ on Callisto appears to be more abundant on the
578 leading hemisphere (Hibbitts *et al.* 2000), opposite to what would be expected from an Io-derived
579 source (and opposite to the distribution of CO₂). Additional features in the Galileo NIMS data also
580 suggest the presence of C-H, S-H, and C≡N, which may play a role in the radiolytic production of
581 CO₂ and possibly SO₂ (McCord *et al.* 1997, 1998; Delitsky & Lane 1998), along with molecular
582 oxygen (Spencer & Calvin 2002), which may represent another trapped species. However, the
583 production of SO₂ and CO₂ and (as for Ganymede) the relative roles of endogenic vs. exogenic
584 processes across different surface materials remain an ongoing question.

585 Observations take above the limb of Callisto by *Galileo* NIMS showed a CO₂ absorption fea-
586 ture, suggesting a tenuous atmosphere with a surface pressure of on the order of 10⁻⁶ Pa (Carl-
587 son 1999). The inferred fast loss rate of CO₂ suggests resupply from surface materials, possibly
588 through the sublimation-degradation process described above. An ionosphere was also detected
589 during the Galileo flybys (Gurnett *et al.* 2000; Kliore *et al.* 2002). Because CO₂ photoionization
590 by itself appears to be insufficient to reproduce the observed electron density, the presence of a
591 significant O₂ atmospheric component has been proposed, (Liang *et al.* 2005) but thus far remains
592 undetected (e.g., see Carberry Mogan *et al.* 2023). More recently, a reanalysis of ultraviolet Hubble
593 Space Telescope observations revealed the presence of a hydrogen exosphere around Callisto, with
594 higher abundances detected when the darker leading hemisphere faces the Sun (Roth *et al.* 2017a).
595 This variation suggests hemispheric differences in the sublimation and release of water-derived
596 species, further highlighting important connections between Callisto's surface composition and its
597 external energy environment.

598 **1.7 Summary and Some Remaining Questions**

599 The four Galilean moons demonstrate the remarkable diversity that can arise from variations in
600 evolutionary pathways, differences in bulk composition and internal evolution, and the range of en-
601 dogenic and exogenic processes that shape planetary and satellite surfaces. Telescopic observations
602 along with the *Voyager* and *Galileo* missions have thus far formed the basis of our understanding
603 of these worlds, but many important questions remain, including:

- 604 • What is the history of the Laplace resonance among Io, Europa, and Ganymede, and how has
605 its timing influenced the long-term thermal evolution of each moon? How has this history in
606 turn shaped the surface geology of each moon?
- 607 • What drives Io's extremely high-temperature mafic volcanism, and what does it reveal about
608 tidal heating, mantle convection, and partial melting processes within the moon? How does
609 Io's interior structure support the sustained volcanic output, and what are the properties of
610 its magma sources? What determining the location, style, and frequency of mantle plumes
611 and volcanic eruptions?
- 612 • What are the chemical and physical properties of Europa's and Ganymede's subsurface
613 oceans. Do these oceans contain the necessary ingredients and energy sources to support
614 biological life? To what extent is there active or past exchange between the subsurface
615 ocean and surface features such as chaos terrain, ridges, or plumes, and how can we detect
616 such exchange today?
- 617 • What are the relative contributions of endogenic (e.g., tectonics, cryovolcanism) vs. exo-
618 genic (e.g., micrometeoroid bombardment, magnetospheric processing) processes in shap-
619 ing the icy surfaces of Europa, Ganymede, and Callisto? What mechanism gives rise to the
620 hydrated mineral component seen at the surfaces of these moons?
- 621 • Why does Ganymede's tectonic record show abundant extension but little or no evidence of
622 compressional features, and what does this imply about its stress history and lithospheric
623 behavior? What is the age of grooved terrain formation on Ganymede, and is there any
624 evidence of continued or episodic activity today?

- 625 • What variations exist in the bulk compositions of Ganyemeade and Callisto inherited from
626 formation? Did Callisto accrete a larger proportion of volatiles such as CO₂ and/or NH₃?
627 What is the internal structure of Callisto, and how does this relate to its relatively quiescent
628 heat production and geologic activity?

629 **References**

- 630 Aksnes, K., 1977. Properties of Satellite Orbits: Ephemerides, Dynamical Constants, and Satellite Phenomena. In
631 *IAU Colloq. 28: Planetary Satellites*. 27
- 632 Anderson, J. D., Jacobson, R. A., Lau, E. L., Moore, W. B. and Schubert, G., 2001a. Io's gravity field and interior
633 structure. *Journal of Geophysical Research*, 106, 32963–32970
- 634 Anderson, J. D., Jacobson, R. A., McElrath, T. P., Moore, W. B., Schubert, G. and Thomas, P. C., 2001b. Shape, Mean
635 Radius, Gravity Field, and Interior Structure of Callisto. *Icarus*, 153, 157–161
- 636 Anderson, J. D., Lau, E. L., Sjogren, W. L., Schubert, G. and Moore, W. B., 1996a. Gravitational constraints on the
637 internal structure of Ganymede. *Nature*, 384, 541–543
- 638 Anderson, J. D., Lau, E. L., Sjogren, W. L., Schubert, G. and Moore, W. B., 1997a. Europa's differentiated internal
639 structure: Inferences from two Galileo encounters. *Science*, 276, 1236–1239
- 640 Anderson, J. D., Lau, E. L., Sjogren, W. L., Schubert, G. and Moore, W. B., 1997b. Gravitational evidence for an
641 undifferentiated Callisto. *Nature*, 387, 264–266
- 642 Anderson, J. D., Null, G. W. and Wong, S. K., 1974. Gravitational Parameters of the Jupiter System from the Doppler
643 Tracking of Pioneer 10. *Science*, 183, 322–323
- 644 Anderson, J. D., Schubert, G., Jacobson, R. A., Lau, E. L., Moore, W. B. and Sjogren, W. L., 1998. Europa's
645 Differentiated Internal Structure: Inferences from Four Galileo Encounters. *Science*, 281, 2019
- 646 Anderson, J. D., Sjogren, W. L. and Schubert, G., 1996b. Galileo Gravity Results and the Internal Structure of Io.
647 *Science*, 272, 709–712
- 648 Bagenal, F., 1994. Empirical model of the Io plasma torus: Voyager measurements. *Journal of Geophysical Research*,
649 99, 11043–11062
- 650 Barnard, E. E., 1895. Jupiter's satellites, filar micrometer measures of, made with the 36-inch equatorial of the Lick
651 Observatory. *Monthly Notices of the Royal Astronomical Society*, 55, 382
- 652 Barth, C. A., Hord, C. W., Stewart, A. I. F., Pryor, W. R., Simmons, K. E., McClintock, W. E., Ajello, J. M., Naviaux,
653 K. L. and Aiello, J. J., 1997. Galileo ultraviolet spectrometer observations of atomic hydrogen in the atmosphere
654 of Ganymede. *Geophysical Research Letters*, 24, 2147–2150
- 655 Belton, M. J. S., Head, I., J. W., Ingersoll, A. P., Greeley, R., McEwen, A. S., Klaasen, K. P., Senske, D., Pappalardo,
656 R., Collins, G., Vasavada, A. R., Sullivan, R., Simonelli, D., Geissler, P., Carr, M. H., Davies, M. E., Veverka,
657 J., Gierasch, P. J., Banfield, D., Bell, M., Chapman, C. R., Anger, C., Greenberg, R., Neukum, G., Pilcher, C. B.,

- 658 Beebe, R. F., Burns, J. A., Fanale, F., Ip, W., Johnson, T. V., Morrison, D., Moore, J., Orton, G. S., Thomas, P. and
659 West, R. A., 1996. Galileo's First Images of Jupiter and the Galilean Satellites. *Science*, 274, 377–385
- 660 Blaney, D. L., Johnson, T. V., Matson, D. L. and Veeder, G. J., 1995. Volcanic eruptions on Io: heat flow, resurfacing,
661 and lava composition. *Icarus*, 113, 220–225
- 662 Blöcker, A., Saur, J., Roth, L. and Strobel, D. F., 2018. MHD Modeling of the Plasma Interaction With Io's Asym-
663 metric Atmosphere. *Journal of Geophysical Research (Space Physics)*, 123, 9286–9311
- 664 Bobis, L. and Lequeux, J., 2008. Cassini, Rømer, and the velocity of light. *Journal of Astronomical History and
665 Heritage*, 11, 97–105
- 666 Breuer, D., Hamilton, C. W. and Khurana, K., 2022. The Internal Structure of Io. *Elements*, 18, 385–390
- 667 Brown, R. A. and Chaffee, J., Frederic H., 1974. High-Resolution Spectra of Sodium Emission from IO. *Astrophysical
668 Journal Letters*, 187, L125
- 669 Calvin, W. M. and Clark, R. N., 1991. Modeling the reflectance spectrum of Callisto 0.25 to 4.1 μm . *Icarus*, 89,
670 305–317
- 671 Calvin, W. M., Clark, R. N., Brown, R. H. and Spencer, J. R., 1995. Spectra of the icy Galilean satellites from 0.2 to 5
672 μm : A compilation, new observations, and a recent summary. *Journal of Geophysical Research*, 100, 19041–19048
- 673 Carberry Mogan, S. R., Liuzzo, L., Poppe, A. R., Simon, S., Szalay, J. R., Tucker, O. J. and Johnson,
674 R. E., 2023. Callisto's atmosphere: The oxygen enigma. *Journal of Geophysical Research: Planets*, 128,
675 e2023JE007894. E2023JE007894 2023JE007894, <https://agupubs.onlinelibrary.wiley.com/doi/pdf/10.1029/2023JE007894>
- 677 Carlson, R. W., 1999. A Tenuous Carbon Dioxide Atmosphere on Jupiter's Moon Callisto. *Science*, 283, 820
- 678 Carlson, R. W., Anderson, M. S., Johnson, R. E., Smythe, W. D., Hendrix, A. R., Barth, C. A., Soderblom, L. A.,
679 Hansen, G. B., McCord, T. B., Dalton, J. B., Clark, R. N., Shirley, J. H., Ocampo, A. C. and Matson, D. L., 1999a.
680 Hydrogen Peroxide on the Surface of Europa. *Science*, 283, 2062
- 681 Carlson, R. W., Bhattacharyya, J. C., Smith, B. A., Johnson, T. V., Hidayat, B., Smith, S. A., Taylor, G. E., O'Leary,
682 B. and Brinkmann, R. T., 1973. An Atmosphere on Ganymede from Its Occultation of SAO 186800 on 7 June
683 1972. *Science*, 182, 53–55
- 684 Carlson, R. W., Calvin, W. M., Dalton, J. B., Hansen, G. B., Hudson, R. L., Johnson, R. E., McCord, T. B. and Moore,
685 M. H., 2009. Europa's Surface Composition. In *Europa* (R. T. Pappalardo, W. B. McKinnon, & K. K. Khurana,
686 eds.). 283

- 687 Carlson, R. W., Johnson, R. E. and Anderson, M. S., 1999b. Sulfuric acid on Europa and the radiolytic sulfur cycle.
688 *Science*, 286, 97–99
- 689 Carr, M. H., 1986. Silicate volcanism on Io. *Journal of Geophysical Research*, 91, 3521–3532
- 690 Carr, M. H., Belton, M. J. S., Chapman, C. R., Davies, M. E., Geissler, P., Greenberg, R., McEwen, A. S., Tufts, B. R.,
691 Greeley, R., Sullivan, R., Head, J. W., Pappalardo, R. T., Klaasen, K. P., Johnson, T. V., Kaufman, J., Senske, D.,
692 Moore, J., Neukum, G., Schubert, G., Burns, J. A., Thomas, P. and Veverka, J., 1998a. Evidence for a subsurface
693 ocean on Europa. *Nature*, 391, 363–365
- 694 Carr, M. H., McEwen, A. S., Howard, K. A., Chuang, F. C., Thomas, P., Schuster, P., Oberst, J., Neukum, G., Schubert,
695 G. and Galileo Imaging Team, 1998b. Mountains and Calderas on Io: Possible Implications for Lithosphere
696 Structure and Magma Generation. *Icarus*, 135, 146–165
- 697 Cartwright, R. J., Villanueva, G. L., Holler, B. J., Camarca, M., Faggi, S., Neveu, M., Roth, L., Raut, U., Glein,
698 C. R., Castillo-Rogez, J. C., Malaska, M. J., Bockelée-Morvan, D., Nordheim, T. A., Hand, K. P., Strazzulla, G.,
699 Pendleton, Y. J., de Kleer, K., Beddingfield, C. B., de Pater, I., Cruikshank, D. P. and Protopapa, S., 2024. Revealing
700 Callisto’s Carbon-rich Surface and CO₂ Atmosphere with JWST. *Planetary Science Journal*, 5, 60. 2401.17236
- 701 Cassen, P. M., Peale, S. J. and Reynolds, R. T., 1981. Structure and Thermal Evolution of the Galilean Satellites. In
702 *IAU Colloq. 57: Satellites of Jupiter* (D. Morrison, ed.), 93
- 703 Cassini, G. D., 1693. *Les hypothèses et les tables des satellites du Jupiter reformées sur de nouvelles observations*
- 704 Clark, R. N., 1980. Ganymede, Europa, Callisto, and Saturn’s rings: Compositional analysis from reflectance spec-
705 troscopy. *Icarus*, 44, 388–409
- 706 Clark, R. N. and McCord, T. B., 1980. The Galilean satellites: New near-infrared spectral reflectance measurements
707 (0.65–2.5 μm) and a 0.325–5 μm summary. *Icarus*, 41, 323–339
- 708 Clow, G. D. and Carr, M. H., 1980. Stability of sulfur slopes on Io. *Icarus*, 44, 268–279
- 709 Collins, G. C., Head, J. W. and Pappalardo, R. T., 1998. Formation of Ganymede Grooved Terrain by Sequential
710 Extensional Episodes: Implications of Galileo Observations for Regional Stratigraphy. *Icarus*, 135, 345–359
- 711 Collins, G. C., Head, J. W., Pappalardo, R. T. and Spaun, N. A., 2000. Evaluation of models for the formation of
712 chaotic terrain on Europa. *Journal of Geophysical Research*, 105, 1709–1716
- 713 Crary, F. J. and Bagenal, F., 1998. Remanent ferromagnetism and the interior structure of Ganymede. *Journal of*
714 *Geophysical Research*, 103, 25757–25774
- 715 Crary, F. J., Bagenal, F., Frank, L. A. and Paterson, W. R., 1998. Galileo plasma spectrometer measurements of
716 composition and temperature in the Io plasma torus. *Journal of Geophysical Research*, 103, 29359–29370

- 717 Cruikshank, D. P. and Morrison, D., 1976. The Galilean satellites of Jupiter. *Scientific American*, 234, 108–116
- 718 Davies, A. G., 2007. *Volcanism on Io*
- 719 Davies, M. E., Colvin, T. R., Oberst, J., Zeitler, W., Schuster, P., Neukum, G., McEwen, A. S., Phillips, C. B., Thomas, P. C., Everka, J., Belton, M. J. S. and Schubert, G., 1998. The Control Networks of the Galilean Satellites and
720 Implications for Global Shape. *Icarus*, 135, 372–376
- 722 de Sitter, W., 1931. Jupiter's Galilean satellites (George Darwin Lecture). *Monthly Notices of the Royal Astronomical Society*, 91, 706–738
- 724 Delamere, P. A. and Bagenal, F., 2003. Modeling variability of plasma conditions in the Io torus. *Journal of Geophysical Research (Space Physics)*, 108, 1276
- 726 Delitsky, M. L. and Lane, A. L., 1998. Ice chemistry on the Galilean satellites. *Journal of Geophysical Research*, 103,
727 31391–31404
- 728 Domingue, D. L. and Lane, A. L., 1998. IUE views Europa: Temporal variations in the UV. *Geophysical Research Letters*, 25, 4421–4424
- 730 Fanale, F. P., Brown, R. H., Cruikshank, D. P. and Clark, R. N., 1979. Significance of absorption features in Io's IR
731 reflectance spectrum. *Nature*, 280, 761–763
- 732 Fanale, F. P., Granahan, J. C., Greeley, R., Pappalardo, R., Head, J., III, Shirley, J., Carlson, R., Hendrix, A., Moore,
733 J., McCord, T. B. and Belton, M., 2000. Tyre and Pwyll: Galileo orbital remote sensing of mineralogy versus
734 morphology at two selected sites on Europa. *Journal of Geophysical Research*, 105, 22647–22657
- 735 Fegley, B. and Zolotov, M. Y., 2000. Chemistry of Sodium, Potassium, and Chlorine in Volcanic Gases on Io. *Icarus*,
736 148, 193–210
- 737 Figueredo, P. H. and Greeley, R., 2004. Resurfacing history of Europa from pole-to-pole geological mapping. *Icarus*,
738 167, 287–312
- 739 Fink, U., Dekkers, N. H. and Larson, H. P., 1973. Infrared Spectra of the Galilean Satellites of Jupiter. *Astrophysical Journal Letters*, 179, L155
- 741 Fischer, H. J. and Spohn, T., 1990. Thermal-orbital histories of viscoelastic models of Io (J1). *Icarus*, 83, 39–65
- 742 Frank, L. A., Ackerson, K. L., Wolfe, J. H. and Mihalov, J. D., 1976. Observations of plasmas in the Jovian magneto-
743 sphere. *Journal of Geophysical Research*, 81, 457
- 744 Frank, L. A., Paterson, W. R., Ackerson, K. L. and Bolton, S. J., 1997. Outflow of hydrogen ions from Ganymede.
745 *Geophysical Research Letters*, 24, 2151–2154

- 746 Galilei, G., 1610. *The sidereal messenger of Galileo Galilei and a part of the preface to Kepler's Dioptrics containing*
747 *the original account of Galileo's astronomical discoveries.* Translation of *Sidereus Nuncius* with Introduction and
748 Notes by Edward Stafford Carlos; London: Rivingtons, 1880.
- 749 Geissler, P., McEwen, A., Phillips, C., Keszthelyi, L. and Spencer, J., 2004. Surface changes on Io during the Galileo
750 mission. *Icarus*, 169, 29–64
- 751 Geissler, P. E., McEwen, A. S., Keszthelyi, L., Lopes-Gautier, R., Granahan, J. and Simonelli, D. P., 1999. Global
752 Color Variations on Io. *Icarus*, 140, 265–282
- 753 Glein, C. R., Baross, J. A. and Waite, J. H., 2015. The pH of Enceladus' ocean. *Geochimica et Cosmochimica Acta*,
754 162, 202–219. 1502.01946
- 755 Goertz, C. K., 1980. Io's interaction with the plasma torus. *Journal of Geophysical Research*, 85, 2949–2956
- 756 Greeley, R., Chyba, C. F., Head, J. W., McCord, T. B., McKinnon, W. B., Pappalardo, R. T., Moore, J. M., Collins,
757 G. C., Kadel, S. D., Hansen, C. J., Hibbitts, C. A. and Prockter, L. M., 2004. Geology of europa. In *Jupiter: The Planet, Satellites and Magnetosphere* (F. Bagenal, T. E. Dowling, & W. B. McKinnon, eds.). Cambridge, UK:
758 Cambridge University Press, 329–362
- 760 Greeley, R., Klemaszewski, J. E., Wagner, R. and Galileo Imaging Team, 2000. Galileo views of the geology of
761 Callisto. *Planetary & Space Science*, 48, 829–853
- 762 Greeley, R., Sullivan, R., Klemaszewski, J., Homan, K., Head, J. W., Pappalardo, R. T., Veverka, J., Clark, B. E., Johnson,
763 T. V., Klaasen, K. P., Belton, M., Moore, J., Asphaug, E., Carr, M. H., Neukum, G., Denk, T., Chapman, C. R.,
764 Pilcher, C. B., Geissler, P. E., Greenberg, R. and Tufts, R., 1998. Europa: Initial Galileo Geological Observations.
765 *Icarus*, 135, 4–24
- 766 Greeley, R., Theilig, E. and Christensen, P., 1984. The Mauna Loa sulfur flow as an analog to secondary sulfur flows
767 (?) on Io. *Icarus*, 60, 189–199
- 768 Greenberg, R., 1977. Orbit-Orbit Resonances among Natural Satellites. In *IAU Colloq. 28: Planetary Satellites*. 157
- 769 Greenberg, R., 1982. Orbital evolution of the Galilean satellites. In *Satellites of Jupiter* (D. Morrison, ed.). 65–92
- 770 Gurnett, D. A., Persoon, A. M., Kurth, W. S., Roux, A. and Bolton, S. J., 2000. Plasma densities in the vicinity of
771 Callisto from Galileo plasma wave observations. *Geophysical Research Letters*, 27, 1867–1870
- 772 Hall, D. T., Feldman, P. D., McGrath, M. A. and Strobel, D. F., 1998. The Far-Ultraviolet Oxygen Airglow of Europa
773 and Ganymede. *Astrophysical Journal*, 499, 475–481
- 774 Hall, D. T., Strobel, D. F., Feldman, P. D., McGrath, M. A. and Weaver, H. A., 1995. Detection of an oxygen
775 atmosphere on Jupiter's moon Europa. *Nature*, 373, 677–679

- 776 Hansen, G. B. and McCord, T. B., 2008. Widespread CO₂ and other non-ice compounds on the anti-Jovian and trailing
777 sides of Europa from Galileo/NIMS observations. *Geophysical Research Letters*, 35, L01202
- 778 Harris, D. L., 1961. Photometry and Colorimetry of Planets and Satellites. In *Planets and Satellites* (G. P. Kuiper &
779 B. M. Middlehurst, eds.). 272
- 780 Hendrix, A. R., Barth, C. A. and Hord, C. W., 1999. Ganymede's ozone-like absorber: Observations by the Galileo
781 ultraviolet spectrometer. *Journal of Geophysical Research*, 104, 14169–14178
- 782 Hendrix, A. R., Barth, C. A., Hord, C. W. and Lane, A. L., 1998. Europa: Disk-Resolved Ultraviolet Measurements
783 Using the Galileo Ultraviolet Spectrometer. *Icarus*, 135, 79–94
- 784 Hendrix, A. R., Cassidy, T. A., Johnson, R. E., Paranicas, C. and Carlson, R. W., 2011. Europa's disk-resolved
785 ultraviolet spectra: Relationships with plasma flux and surface terrains. *Icarus*, 212, 736–743
- 786 Herschel, W., 1797. Observations of the Changeable Brightness of the Satellites of Jupiter, and of the Variation in
787 Their Apparent Magnitudes; With a Determination of the Time of Their Rotatory Motions on Their Axes. To Which
788 is Added, a Measure of the Diameter of the Second Satellite, and an Estimate of the Comparative Size of All the
789 Four. By William Herschel, LL.D. F. R. S. *Philosophical Transactions of the Royal Society of London Series I*, 87,
790 332–351
- 791 Hibbitts, C. A., Klemaszewski, J. E., McCord, T. B., Hansen, G. B. and Greeley, R., 2002. CO₂-rich impact craters
792 on Callisto. *Journal of Geophysical Research (Planets)*, 107, 5084
- 793 Hibbitts, C. A., McCord, T. B. and Hansen, G. B., 2000. Distributions of CO₂ and SO₂ on the surface of Callisto.
794 *Journal of Geophysical Research*, 105, 22541–22558
- 795 Hogenboom, D. L., Kargel, J. S., Consolmagno, G. J., Holden, T. C., Lee, L. and Buuyounouski, M., 1997. The
796 Ammonia-Water System and the Chemical Differentiation of Icy Satellites. *Icarus*, 128, 171–180
- 797 Houzeau, J.-C., 1882. *Tables écliptiques des satellites de Jupiter*. Brussels: F. Hayez, Imprimeur de L'académie
798 Royale de Belgique
- 799 Hussmann, H. and Spohn, T., 2004. Thermal-orbital evolution of Io and Europa. *Icarus*, 171, 391–410
- 800 Hussmann, H., Spohn, T. and Wieczorkowski, K., 2002. Thermal Equilibrium States of Europa's Ice Shell: Implica-
801 tions for Internal Ocean Thickness and Surface Heat Flow. *Icarus*, 156, 143–151
- 802 Intriligator, D. S. and Miller, W. D., 1981. Detection of the Io plasma torus by Pioneer 10. *Geophysical Research
803 Letters*, 8, 409–412
- 804 Jessup, K. L. and Spencer, J. R., 2015. Spatially resolved HST/STIS observations of Io's dayside equatorial atmo-
805 sphere. *Icarus*, 248, 165–189

- 806 Jia, X., Kivelson, M. G., Khurana, K. K. and Kurth, W. S., 2018. Evidence of a plume on Europa from Galileo
807 magnetic and plasma wave signatures. *Nature Astronomy*, 2, 459–464
- 808 Jia, X., Kivelson, M. G. and Paranicas, C., 2021. Comment on “an active plume eruption on europa during
809 galileo flyby e26 as indicated by energetic proton depletions” by huybrighs et al. *Geophysical Research Letters*,
810 48, e2020GL091550. E2020GL091550 2020GL091550, <https://agupubs.onlinelibrary.wiley.com/doi/pdf/10.1029/2020GL091550>
- 812 Johnson, R. E., Burger, M. H., Cassidy, T. A., Leblanc, F., Marconi, M. and Smyth, W. H., 2009. Composition
813 and Detection of Europa’s Sputter-induced Atmosphere. In *Europa* (R. T. Pappalardo, W. B. McKinnon, & K. K.
814 Khurana, eds.). 507
- 815 Johnson, T. V., 2014. Major Satellites of the Giant Planets. In *Planets, Asteroids, Comets and The Solar System*,
816 volume 2 (A. M. Davis, ed.). 313–334
- 817 Johnson, T. V. and Pilcher, C. B., 1977. Satellite Spectrophotometry and Surface Compositions. In *IAU Colloq. 28: Planetary Satellites*. 232
- 819 Johnson, T. V., Soderblom, L. A., Mosher, J. A., Danielson, G. E., Cook, A. F. and Kupperman, P., 1983. Global
820 multispectral mosaics of the icy Galilean satellites. *Journal of Geophysical Research*, 88, 5789–5805
- 821 Johnson, T. V., Veeder, G. J., Matson, D. L., Brown, R. H., Nelson, R. M. and Morrison, D., 1988. Io: Evidence for
822 Silicate Volcanism in 1986. *Science*, 242, 1280–1283
- 823 Journaux, B., Daniel, I., Petitgirard, S., Cardon, H., Perrillat, J.-P., Caracas, R. and Mezouar, M., 2017. Salt par-
824 titioning between water and high-pressure ices. Implication for the dynamics and habitability of icy moons and
825 water-rich planetary bodies. *Earth and Planetary Science Letters*, 463, 36–47
- 826 Kargel, J. S., 1992. Ammonia-water volcanism on icy satellites: Phase relations at 1 atmosphere. *Icarus*, 100, 556–574
- 827 Kargel, J. S., Croft, S. K., Lunine, J. I. and Lewis, J. S., 1991. Rheological properties of ammonia-water liquids and
828 crystal-liquid slurries: Planetological applications. *Icarus*, 89, 93–112
- 829 Kargel, J. S., Kaye, J. Z., Head, J. W., Marion, G. M., Sassen, R., Crowley, J. K., Ballesteros, O. P., Grant, S. A. and
830 Hogenboom, D. L., 2000. Europa’s Crust and Ocean: Origin, Composition, and the Prospects for Life. *Icarus*, 148,
831 226–265
- 832 Keszthelyi, L., McEwen, A. S., Phillips, C. B., Milazzo, M., Geissler, P., Turtle, E. P., Radebaugh, J., Williams, D. A.,
833 Simonelli, D. P., Breneman, H. H., Klaasen, K. P., Levanas, G. and Denk, T., 2001. Imaging of volcanic activity
834 on jupiter’s moon io by galileo during the galileo europa mission and the galileo millennium mission. *Journal
835 of Geophysical Research: Planets*, 106, 33025–33052. <https://agupubs.onlinelibrary.wiley.com/doi/pdf/10.1029/2000JE001383>

- 837 Khurana, K. K., Jia, X., Kivelson, M. G., Nimmo, F., Schubert, G. and Russell, C. T., 2011. Evidence of a Global
838 Magma Ocean in Io's Interior. *Science*, 332, 1186
- 839 Khurana, K. K., Kivelson, M. G., Stevenson, D. J., Schubert, G., Russell, C. T., Walker, R. J. and Polanskey, C., 1998.
840 Induced magnetic fields as evidence for subsurface oceans in Europa and Callisto. *Nature*, 395, 777–780
- 841 Kivelson, M. G., Khurana, K. K., Russell, C. T., Joy, S. P., Volwerk, M., Walker, R. J., Zimmer, C. and Linker, J. A.,
842 2001. Magnetized or unmagnetized: Ambiguity persists following Galileo's encounters with Io in 1999 and 2000.
843 *Journal of Geophysical Research*, 106, 26121–26136
- 844 Kivelson, M. G., Khurana, K. K., Russell, C. T., Volwerk, M., Walker, R. J. and Zimmer, C., 2000. Galileo Magne-
845 tometer Measurements: A Stronger Case for a Subsurface Ocean at Europa. *Science*, 289, 1340–1343
- 846 Kivelson, M. G., Khurana, K. K., Russell, C. T., Walker, R. J., Warnecke, J., Coroniti, F. V., Polanskey, C., Southwood,
847 D. J. and Schubert, G., 1996a. Discovery of Ganymede's magnetic field by the Galileo spacecraft. *Nature*, 384,
848 537–541
- 849 Kivelson, M. G., Khurana, K. K., Stevenson, D. J., Bennett, L., Joy, S., Russell, C. T., Walker, R. J., Zimmer, C. and
850 Polanskey, C., 1999. Europa and Callisto: Induced or intrinsic fields in a periodically varying plasma environment.
851 *Journal of Geophysical Research*, 104, 4609–4626
- 852 Kivelson, M. G., Khurana, K. K. and Volwerk, M., 2002. The Permanent and Inductive Magnetic Moments of
853 Ganymede. *Icarus*, 157, 507–522
- 854 Kivelson, M. G., Khurana, K. K., Walker, R. J., Warnecke, J., Russell, C. T., Linker, J. A., Southwood, D. J. and
855 Polanskey, C., 1996b. Io's Interaction with the Plasma Torus: Galileo Magnetometer Report. *Science*, 274, 396–
856 398
- 857 Kliore, A. J., Anabtawi, A., Herrera, R. G., Asmar, S. W., Nagy, A. F., Hinson, D. P. and Flasar, F. M., 2002. Iono-
858 sphere of Callisto from Galileo radio occultation observations. *Journal of Geophysical Research (Space Physics)*,
859 107, 1407
- 860 Kuiper, G. P., 1957. Infrared observations of planets and satellites. *Astronomical Journal*, 62, 245–245
- 861 Kumar, S. and Hunten, D. M., 1982. The atmospheres of Io and other satellites. In *Satellites of Jupiter* (D. Morrison,
862 ed.). 782–806
- 863 Kupo, I., Mekler, Y., Mekler, Y. and Eviatar, A., 1976. Detection of ionized sulfur in the Jovian magnetosphere.
864 *Astrophysical Journal Letters*, 205, L51–L53
- 865 Lane, A. L. and Domingue, D. L., 1997. IUE's View of Callisto: Detection of an SO₂ Absorption Correlated to
866 Possible Torus Neutral Wind Alterations. *Geophysical Research Letters*, 24, 1143

- 867 Laplace, P.-S., 1805. *Traité de Mécanique Céleste* (Vol. IV) . Paris: Chez Courcier
- 868 Lebofsky, L. A., 1975. Stability of Frosts in the Solar System. *Icarus*, 25, 205–217
- 869 Lebofsky, L. A. and Feierberg, M. A., 1985. 2.7- to 4.1- μ m spectrophotometry of icy satellites of Saturn and Jupiter.
- 870 *Icarus*, 63, 237–242
- 871 Leith, A. C. and McKinnon, W. B., 1996. Is There Evidence for Polar Wander on Europa? *Icarus*, 120, 387–398
- 872 Lewis, J. S., 1971a. Satellites of the Outer Planets: Their Physical and Chemical Nature. *Icarus*, 15, 174–185
- 873 Lewis, J. S., 1971b. Satellites of the Outer Planets: Thermal Models. *Science*, 172, 1127–1128
- 874 Liang, M.-C., Lane, B. F., Pappalardo, R. T., Allen, M. and Yung, Y. L., 2005. Atmosphere of Callisto. *Journal of*
- 875 *Geophysical Research (Planets)*, 110, E02003
- 876 Lieske, J. H., 1987. Galilean satellite evolution - Observational evidence for secular changes in mean motions. *Ast-*
- 877 *ronomy & Astrophysics*, 176, 146–158
- 878 Lodders, K. and Fegley, B., Jr., 1998. *The Planetary Scientist's Companion*. New York: Oxford Univ. Press
- 879 Lopes, R. M. C., 2007. Io. The Volcanic Moon. In *Encyclopedia of the Solar System* (L. A. A. McFadden, P. R.
- 880 Weissman, & T. V. Johnson, eds.). 419–430
- 881 Lopes, R. M. C., Kamp, L. W., Smythe, W. D., Mouginis-Mark, P., Kargel, J., Radebaugh, J., Turtle, E. P., Perry, J.,
- 882 Williams, D. A., Carlson, R. W., Douté, S., the Galileo NIMS and SSI Teams, 2004. Lava lakes on Io: observations
- 883 of Io's volcanic activity from Galileo NIMS during the 2001 fly-bys. *Icarus*, 169, 140–174
- 884 Lopes, R. M. C. and Spencer, J. R., 2007. *Io After Galileo: A New View of Jupiter's Volcanic Moon*
- 885 Lopes-Gautier, R., McEwen, A. S., Smythe, W. B., Geissler, P. E., Kamp, L., Davies, A. G., Spencer, J. R., Keszthelyi,
- 886 L., Carlson, R., Leader, F. E., Mehlman, R., Soderblom, L., The Galileo NIMS and SSI Teams, 1999. Active
- 887 Volcanism on Io: Global Distribution and Variations in Activity. *Icarus*, 140, 243–264
- 888 Lucchitta, B. K. and Soderblom, L. A., 1982. The geology of Europa. In *Satellites of Jupiter* (D. Morrison, ed.).
- 889 521–555
- 890 Lunine, J. I. and Stevenson, D. J., 1985. Thermodynamics of clathrate hydrate at low and high pressures with applica-
- 891 tion to the outer solar system. *Astrophysical Journal Supplement*, 58, 493–531
- 892 Malhotra, R., 1991. Tidal origin of the Laplace resonance and the resurfacing of Ganymede. *Icarus*, 94, 399–412
- 893 Matsuyama, I. N., Steinke, T. and Nimmo, F., 2022. Tidal Heating in Io. *Elements*, 18, 374–378

- 894 Mauk, B. H., Mitchell, D. G., Krimigis, S. M., Roelof, E. C. and Paranicas, C. P., 2003. Energetic neutral atoms from
895 a trans-Europa gas torus at Jupiter. *Nature*, 421, 920–922
- 896 McCarthy, C. and Cooper, R. F., 2016. Tidal dissipation in creeping ice and the thermal evolution of Europa. *Earth*
897 and *Planetary Science Letters*, 443, 185–194
- 898 McCord, T. B., Carlson, R., Smythe, W., Hansen, G., Clark, R., Hibbitts, C., Fanale, F., Granahan, J., Segura, M., Mat-
899 son, D., Johnson, T. and Martin, P., 1997. Organics and other molecules in the surfaces of Callisto and Ganymede.
900 *Science*, 278, 271–275
- 901 McCord, T. B., Hansen, G. B., Clark, R. N., Martin, P. D., Hibbitts, C. A., Fanale, F. P., Granahan, J. C., Segura, M.,
902 Matson, D. L., Johnson, T. V., Carlson, R. W., Smythe, W. D. and Danielson, G. E., 1998. Non-water-ice con-
903 stituents in the surface material of the icy Galilean satellites from the Galileo near-infrared mapping spectrometer
904 investigation. *Journal of Geophysical Research*, 103, 8603–8626
- 905 McCord, T. B., Hansen, G. B. and Hibbitts, C. A., 2001. Hydrated Salt Minerals on Ganymede's Surface: Evidence
906 of an Ocean Below. *Science*, 292, 1523–1525
- 907 McCord, T. B., Hansen, G. B., Matson, D. L., Jonhson, T. V., Crowley, J. K., Fanale, F. P., Carlson, R. W., Smythe,
908 W. D., Martin, P. D., Hibbitts, C. A., Granahan, J. C. and Ocampo, A., 1999. Hydrated salt minerals on Eu-
909 ropa's surface from the Galileo near-infrared mapping spectrometer (NIMS) investigation. *Journal of Geophysical*
910 *Research*, 104, 11827–11852
- 911 McEwen, A. S., Keszthelyi, L., Spencer, J. R., Schubert, G., Matson, D. L., Lopes-Gautier, R., Klaasen, K. P., Johnson,
912 T. V., Head, J. W., Geissler, P., Fagents, S., Davies, A. G., Carr, M. H., Breneman, H. H. and Belton, M. J. S., 1998.
913 High-Temperature Silicate Volcanism on Jupiter's Moon Io. *Science*, 281, 87
- 914 McFadden, L. A., Bell, J. F. and McCord, T. B., 1980. Visible spectral reflectance measurements (0.33–1.1 μm) of the
915 Galilean satellites at many orbital phase angles. *Icarus*, 44, 410–430
- 916 McGrath, M. A., 2014. The Giant Planet Satellite Exospheres. In *AGU Fall Meeting Abstracts*, volume 2014. P21F–07
- 917 McKinnon, W. B., 1997. NOTE: Mystery of Callisto: Is It Undifferentiated? *Icarus*, 130, 540–543
- 918 McKinnon, W. B. and Melosh, H. J., 1980. Evolution of planetary lithospheres: Evidence from multiringed structures
919 on Ganymede and Callisto. *Icarus*, 44, 454–471
- 920 McKinnon, W. B. and Parmentier, E. M., 1986. Ganymede and Callisto. In *IAU Colloq. 77: Some Background about*
921 *Satellites* (J. A. Burns & M. S. Matthews, eds.). 718–763

- 922 Moore, J. M., Asphaug, E., Belton, M. J. S., Bierhaus, B., Breneman, H. H., Brooks, S. M., Chapman, C. R., Chuang,
923 F. C., Collins, G. C., Giese, B., Greeley, R., Head, J. W., Kadel, S., Klaasen, K. P., Klemaszewski, J. E., Magee,
924 K. P., Moreau, J., Morrison, D., Neukum, G., Pappalardo, R. T., Phillips, C. B., Schenk, P. M., Senske, D. A.,
925 Sullivan, R. J., Turtle, E. P. and Williams, K. K., 2001. Impact Features on Europa: Results of the Galileo Europa
926 Mission (GEM). *Icarus*, 151, 93–111
- 927 Moore, J. M., Asphaug, E., Morrison, D., Spencer, J. R., Chapman, C. R., Bierhaus, B., Sullivan, R. J., Chuang, F. C.,
928 Klemaszewski, J. E., Greeley, R., Bender, K. C., Geissler, P. E., Helfenstein, P. and Pilcher, C. B., 1999. Mass
929 Movement and Landform Degradation on the Icy Galilean Satellites: Results of the Galileo Nominal Mission.
930 *Icarus*, 140, 294–312
- 931 Moore, J. M., Asphaug, E., Sullivan, R. J., Klemaszewski, J. E., Bender, K. C., Greeley, R., Geissler, P. E., McEwen,
932 A. S., Turtle, E. P., Phillips, C. B., Tufts, B. R., Head, J. W., Pappalardo, R. T., Jones, K. B., Chapman, C. R.,
933 Belton, M. J. S., Kirk, R. L. and Morrison, D., 1998. Large Impact Features on Europa: Results of the Galileo
934 Nominal Mission. *Icarus*, 135, 127–145
- 935 Moore, J. M., Chapman, C. R., Bierhaus, E. B., Greeley, R., Chuang, F. C., Klemaszewski, J., Clark, R. N., Dalton,
936 J. B., Hibbitts, C. A., Schenk, P. M., Spencer, J. R. and Wagner, R., 2004. Callisto. In *Jupiter. The Planet, Satellites*
937 and *Magnetosphere*, volume 1 (F. Bagenal, T. E. Dowling, & W. B. McKinnon, eds.). 397–426
- 938 Morabito, L. A., Synnott, S. P., Kupferman, P. N. and Collins, S. A., 1979. Discovery of Currently Active Extraterrestrial
939 Volcanism. *Science*, 204, 972
- 940 Moroz, V. I., 1961. On the Infrared Spectra of Jupiter and Saturn (0.9–2.5 μm). *Astronomicheskii Zhurnal*, 38, 1080
- 941 Morrison, D., 1982. Introduction to the satellites of Jupiter. In *Satellites of Jupiter*. 3–43
- 942 Morrison, D., Cruikshank, D. P. and Burns, J. A., 1977. Introducing the Satellites. In *IAU Colloq. 28: Planetary*
943 *Satellites*. 3
- 944 Moses, J. I., Zolotov, M. Y. and Fegley, B., 2002a. Alkali and Chlorine Photochemistry in a Volcanically Driven
945 Atmosphere on Io. *Icarus*, 156, 107–135
- 946 Moses, J. I., Zolotov, M. Y. and Fegley, B., 2002b. Photochemistry of a Volcanically Driven Atmosphere on Io: Sulfur
947 and Oxygen Species from a Pele-Type Eruption. *Icarus*, 156, 76–106
- 948 Mousis, O. and Alibert, Y., 2006. Modeling the Jovian subnebula. II. Composition of regular satellite ices. *Astronomy*
949 & *Astrophysics*, 448, 771–778. [astro-ph/0510798](#)
- 950 Murchie, S. L., Head, J. W., Helfenstein, P. and Plescia, J. B., 1986. Terrain types and local-scale stratigraphy of
951 grooved terrain on Ganymede. *Journal of Geophysical Research*, 91, E222–E238

- 952 Nagel, K., Breuer, D. and Spohn, T., 2004. A model for the interior structure, evolution, and differentiation of Callisto.
953 *Icarus*, 169, 402–412
- 954 Nelson, M. L., McCord, T. B., Clark, R. N., Johnson, T. V., Matson, D. L., Mosher, J. A. and Soderblom, L. A., 1986.
955 Europa: Characterization and interpretation of global spectral surface units. *Icarus*, 65, 129–151
- 956 Nelson, R. M., Lane, A. L., Matson, D. L., Veeder, G. J., Buratti, B. J. and Tedesco, E. F., 1987. Spectral geometric
957 albedos of the Galilean satellites from 0.24 to 0.34 micrometers: Observations with the international ultraviolet
958 explorer. *Icarus*, 72, 358–380
- 959 Neubauer, F. M., 1998. The sub-Alfvénic interaction of the Galilean satellites with the Jovian magnetosphere. *Journal
960 of Geophysical Research*, 103, 19843–19866
- 961 Nimmo, F., Thomas, P. C., Pappalardo, R. T. and Moore, W. B., 2007. The global shape of Europa: Constraints on
962 lateral shell thickness variations. *Icarus*, 191, 183–192
- 963 Noll, K. S., Johnson, R. E., Lane, A. L., Domingue, D. L. and Weaver, H. A., 1996. Detection of Ozone on Ganymede.
964 *Science*, 273, 341–343
- 965 Noll, K. S., Johnson, R. E., McGrath, M. A. and Caldwell, J. J., 1997. Detection of SO₂ on Callisto with the Hubble
966 Space Telescope. *Geophysical Research Letters*, 24, 1139–1142
- 967 Noll, K. S., Weaver, H. A. and Gonnella, A. M., 1995. The albedo spectrum of Europa from 2200 Å to 3300 Å.
968 *Journal of Geophysical Research*, 100, 19057–19060
- 969 Ojakangas, G. W. and Stevenson, D. J., 1986. Episodic volcanism of tidally heated satellites with application to Io.
970 *Icarus*, 66, 341–358
- 971 Paganini, L., Villanueva, G. L., Roth, L., Mandell, A. M., Hurford, T. A., Retherford, K. D. and Mumma, M. J., 2020.
972 A measurement of water vapour amid a largely quiescent environment on Europa. *Nature Astronomy*, 4, 266–272
- 973 Pappalardo, R. T., Belton, M. J. S., Breneman, H. H., Carr, M. H., Chapman, C. R., Collins, G. C., Denk, T., Fagents,
974 S., Geissler, P. E., Giese, B., Greeley, R., Greenberg, R., Head, J. W., Helfenstein, P., Hoppa, G., Kadel, S. D.,
975 Klaasen, K. P., Klemaszewski, J. E., Magee, K., McEwen, A. S., Moore, J. M., Moore, W. B., Neukum, G.,
976 Phillips, C. B., Prockter, L. M., Schubert, G., Senske, D. A., Sullivan, R. J., Tufts, B. R., Turtle, E. P., Wagner, R.
977 and Williams, K. K., 1999. Does Europa have a subsurface ocean? Evaluation of the geological evidence. *Journal
978 of Geophysical Research*, 104, 24015–24056
- 979 Pappalardo, R. T., Buratti, B. J., Korth, H. et al, 2024. Science Overview of the Europa Clipper Mission. *Space
980 Science Reviews*, 220, 40

- 981 Pappalardo, R. T., Collins, G. C., Head, J. W., III, Helfenstein, P., McCord, T. B., Moore, J. M., Prockter, L. M.,
982 Schenk, P. M. and Spencer, J. R., 2004. Geology of Ganymede. In *Jupiter: The Planet, Satellites and Magnetosphere*, volume 1 (F. Bagenal, T. E. Dowling, & W. B. McKinnon, eds.). 363–396
- 984 Pappalardo, R. T., Head, J. W., Collins, G. C., Kirk, R. L., Neukum, G., Oberst, J., Giese, B., Greeley, R., Chapman,
985 C. R., Helfenstein, P., Moore, J. M., McEwen, A., Tufts, B. R., Senske, D. A., Breneman, H. H. and Klaasen, K.,
986 1998a. Grooved Terrain on Ganymede: First Results from Galileo High-Resolution Imaging. *Icarus*, 135, 276–302
- 987 Pappalardo, R. T., Head, J. W., Greeley, R., Sullivan, R. J., Pilcher, C., Schubert, G., Moore, W. B., Carr, M. H., Moore,
988 J. M., Belton, M. J. S. and Goldsby, D. L., 1998b. Geological evidence for solid-state convection in Europa's ice
989 shell. *Nature*, 391, 365–368
- 990 Peale, S. J., Cassen, P. and Reynolds, R. T., 1979. Melting of Io by Tidal Dissipation. *Science*, 203, 892–894
- 991 Pearl, J., Hanel, R., Kunde, V., Maguire, W., Fox, K., Gupta, S., Ponnامperuma, C. and Raulin, F., 1979. Identification
992 of gaseous SO₂ and new upper limits for other gases on Io. *Nature*, 280, 755–758
- 993 Pearl, J. C. and Sinton, W. M., 1982. Hot spots of Io. In *Satellites of Jupiter* (D. Morrison, ed.). 724–755
- 994 Pickering, E. C., Searle, A. and Upton, W., 1879. Photometric Observations. Part II. Chapter VIII. Satellites of Jupiter.
995 *Annals of Harvard College Observatory*, 11, 239–246
- 996 Pilcher, C. B., Ridgway, S. T. and McCord, T. B., 1972. Galilean Satellites: Identification of Water Frost. *Science*,
997 178, 1087–1089
- 998 Pollack, J. B. and Fanale, F., 1982. Origin and evolution of the Jupiter satellite system. In *Satellites of Jupiter*. 872–910
- 999 Pollack, J. B., Witteborn, F. C., Erickson, E. F., Strecker, D. W., Baldwin, B. J. and Bunch, T. E., 1978. Near-infrared
1000 spectra of the Galilean satellites: Observations and compositional implications. *Icarus*, 36, 271–303
- 1001 Prickard, A., 1916. The Mundus Jovialis of Simon Marius (English translation of 1614 edition). *The Observatory*, 39,
1002 367–381
- 1003 Prockter, L. M., Head, J. W., Pappalardo, R. T., Senske, D. A., Neukum, G., Wagner, R., Wolf, U., Oberst, J. O., Giese,
1004 B., Moore, J. M., Chapman, C. R., Helfenstein, P., Greeley, R., Breneman, H. H. and Belton, M. J. S., 1998. Dark
1005 Terrain on Ganymede: Geological Mapping and Interpretation of Galileo Regio at High Resolution. *Icarus*, 135,
1006 317–344
- 1007 Prockter, L. M., Head, J. W., Pappalardo, R. T., Sullivan, R. J., Clifton, A. E., Giese, B., Wagner, R. and Neukum,
1008 G., 2002. Morphology of Europan bands at high resolution: A mid-ocean ridge-type rift mechanism. *Journal of
1009 Geophysical Research (Planets)*, 107, 5028

- 1010 Quick, L. C., Barnouin, O. S., Prockter, L. M. and Patterson, G. W., 2013. Constraints on the detection of cryovolcanic
1011 plumes on Europa. *Planetary and Space Science*, 86, 1–9
- 1012 Rathbun, J. A., Musser, G. S., Jr. and Squyres, S. W., 1998. Ice diapirs on Europa: Implications for liquid water.
1013 *Geophysical Research Letters*, 25, 4157–4160
- 1014 Reynolds, R. T. and Cassen, P. M., 1979. On the internal structure of the major satellites of the outer planets. *Geo-*
1015 *physical Research Letters*, 6, 121–124
- 1016 Reynolds, R. T., Squyres, S. W., Colburn, D. S. and McKay, C. P., 1983. On the habitability of Europa. *Icarus*, 56,
1017 246–254
- 1018 Roth, L., Alday, J., Becker, T. M., Ivchenko, N. and Retherford, K. D., 2017a. Detection of a hydrogen corona at
1019 Callisto. *Journal of Geophysical Research (Planets)*, 122, 1046–1055
- 1020 Roth, L., Retherford, K. D., Ivchenko, N., Schlatter, N., Strobel, D. F., Becker, T. M. and Grava, C., 2017b. Detection
1021 of a Hydrogen Corona in HST Ly α Images of Europa in Transit of Jupiter. *Astronomical Journal*, 153, 67
- 1022 Roth, L., Saur, J., Retherford, K. D., Strobel, D. F., Feldman, P. D., McGrath, M. A. and Nimmo, F., 2014. Transient
1023 Water Vapor at Europa's South Pole. *Science*, 343, 171–174
- 1024 Roush, T. L., Pollack, J. B., Witteborn, F. C., Bregman, J. D. and Simpson, J. P., 1990. Ice and minerals on Callisto:
1025 A reassessment of the reflectance spectra. *Icarus*, 86, 355–382
- 1026 Rückriemen, T., Breuer, D. and Spohn, T., 2018. Top-down freezing in a Fe-FeS core and Ganymede's present-day
1027 magnetic field. *Icarus*, 307, 172–196
- 1028 Sagan, C., 1979. Sulphur flows on Io. *Nature*, 280, 750–753
- 1029 Sampson, R. A., 1921. Theory of the Four Great Satellites of Jupiter. *Memoirs of the Royal Astronomical Society*, 63,
1030 1
- 1031 Schenk, P., Hargitai, H., Wilson, R., McEwen, A. and Thomas, P., 2001. The mountains of Io: Global and geological
1032 perspectives from Voyager and Galileo. *Journal of Geophysical Research*, 106, 33201–33222
- 1033 Schenk, P., Matsuyama, I. and Nimmo, F., 2008. True polar wander on Europa from global-scale small-circle depres-
1034 sions. *Nature*, 453, 368–371
- 1035 Schenk, P. M., 1991. Ganymede and Callisto: Complex crater formation and planetary crusts. *Journal of Geophysical
1036 Research*, 96, 15635–15664
- 1037 Schenk, P. M., 1995. The Geology of Callisto. *Journal of Geophysical Research*, 100, 19023–19040

- 1038 Schenk, P. M., 2002. Thickness constraints on the icy shells of the galilean satellites from a comparison of crater
1039 shapes. *Nature*, 417, 419–421
- 1040 Schenk, P. M. and Bulmer, M. H., 1998. Origin of Mountains on Io by Thrust Faulting and Large-Scale Mass Move-
1041 ments. *Science*, 279, 1514
- 1042 Schubert, G., Anderson, J. D., Spohn, T. and McKinnon, W. B., 2004. Interior composition, structure and dynamics
1043 of the galilean satellites. In *Jupiter: The Planet, Satellites and Magnetosphere* (F. Bagenal, T. E. Dowling, & W. B.
1044 McKinnon, eds.). Cambridge, UK: Cambridge University Press, 281–306
- 1045 Schubert, G., Stevenson, D. J. and Ellsworth, K., 1981. Internal structures of the Galilean satellites. *Icarus*, 47, 46–59
- 1046 Schubert, G., Zhang, K., Kivelson, M. G. and Anderson, J. D., 1996. The magnetic field and internal structure of
1047 Ganymede. *Nature*, 384, 544–545
- 1048 Secchi, A., 1856. Schreiben des Herrn Professors Secchi, Directors der Sternwarte des Coll. Rom., an den Herausge-
1049 ber. *Astronomische Nachrichten*, 43, 135
- 1050 Segatz, M., Spohn, T., Ross, M. N. and Schubert, G., 1988. Tidal dissipation, surface heat flow, and figure of vis-
1051 coelastic models of Io. *Icarus*, 75, 187–206
- 1052 Shoemaker, E. M., Lucchitta, B. K., Wilhelms, D. E., Plescia, J. B. and Squyres, S. W., 1982. The geology of
1053 Ganymede. In *Satellites of Jupiter* (D. Morrison, ed.). 435–520
- 1054 Showman, A. P. and Malhotra, R., 1997. Tidal Evolution into the Laplace Resonance and the Resurfacing of
1055 Ganymede. *Icarus*, 127, 93–111
- 1056 Showman, A. P. and Malhotra, R., 1999. The Galilean satellites. *Science*, 296, 77–84
- 1057 Showman, A. P., Stevenson, D. J. and Malhotra, R., 1997. Coupled Orbital and Thermal Evolution of Ganymede.
1058 *Icarus*, 129, 367–383
- 1059 Sill, G. T. and Clark, R. N., 1982. Composition of the surfaces of the Galilean satellites. In *Satellites of Jupiter*.
1060 174–212
- 1061 Smith, B. A., Soderblom, L. A., Beebe, R., Boyce, J., Briggs, G., Carr, M., Collins, S. A., Cook, I., Allan F., Danielson,
1062 G. E., Davies, M. E., Hunt, G. E., Ingersoll, A., Johnson, T. V., Masursky, H., McCauley, J., Morrison, D., Owen,
1063 T., Sagan, C., Shoemaker, E. M., Strom, R., Suomi, V. E. and Veverka, J., 1979a. The Galilean Satellites and
1064 Jupiter: Voyager 2 Imaging Science Results. *Science*, 206, 927–950
- 1065 Smith, B. A., Soderblom, L. A., Johnson, T. V., Ingersoll, A. P., Collins, S. A., Shoemaker, E. M., Hunt, G. E.,
1066 Masursky, H., Carr, M. H., Davies, M. E., Cook, I., Allan F., Boyce, J., Danielson, G. E., Owen, T., Sagan, C.,

- 1067 Beebe, R. F., Veverka, J., Strom, R. G., McCauley, J. F., Morrison, D., Briggs, G. A. and Suomi, V. E., 1979b. The
1068 Jupiter System Through the Eyes of Voyager 1. *Science*, 204, 951–957
- 1069 Smith, P. H., 1978. Diameters of the Galilean satellites from pioneer data. *Icarus*, 35, 167–176
- 1070 Smythe, W. D., Carlson, R. W., Ocampo, A., Matson, D., Johnson, T. V., McCord, T. B., Hansen, G. E., Soderblom,
1071 L. A. and Clark, R. N., 1998. Absorption Bands in the Spectrum of Europa Detected by the Galileo NIMS Instru-
1072 ment. In *Lunar and Planetary Science Conference*, Lunar and Planetary Science Conference. 1532
- 1073 Spencer, J. R. and Calvin, W. M., 2002. Condensed O₂ on Europa and Callisto. *Astronomical Journal*, 124, 3400–3403
- 1074 Spencer, J. R., Calvin, W. M. and Person, M. J., 1995. CCD Spectra of the Galilean Satellites: Molecular Oxygen on
1075 Ganymede. *Journal of Geophysical Research*, 100, 19049–19056
- 1076 Spencer, J. R. and Maloney, P. R., 1984. Mobility of water ice on callisto: Evidence and implications. *Geophys-
1077 ical Research Letters*, 11, 1223–1226. [https://agupubs.onlinelibrary.wiley.com/doi/pdf/10.1029/
1078 GL011i012p01223](https://agupubs.onlinelibrary.wiley.com/doi/pdf/10.1029/GL011i012p01223)
- 1079 Spencer, J. R. and Schneider, N. M., 1996. Io on the Eve of the Galileo Mission. *Annual Review of Earth and
1080 Planetary Sciences*, 24, 125–190
- 1081 Spohn, T. and Schubert, G., 2003. Oceans in the icy Galilean satellites of Jupiter? *Icarus*, 161, 456–467
- 1082 Squyres, S. W., 1980. Surface temperatures and retention of H₂O frost on Ganymede and Callisto. *Icarus*, 44,
1083 502–510
- 1084 Stebbins, J., 1927. The light-variations of the satellites of Jupiter and their application to measures of the solar constant.
1085 *Lick Observatory Bulletin*, 385, 1
- 1086 Stebbins, J. and Jacobsen, T. S., 1928. Further photometric measures of Jupiter's satellites and Uranus, with tests of
1087 the solar constant. *Lick Observatory Bulletin*, 401, 180–195
- 1088 Strom, R. G. and Schneider, N. M., 1982. Volcanic eruption plumes on Io. In *Satellites of Jupiter*. 598–633
- 1089 Strom, R. G., Terrile, R. J., Masursky, H. and Hansen, C., 1979. Volcanic eruption plumes on Io. *Nature*, 280, 733–736
- 1090 Taylor, G. E., 1972. The Determination of the Diameter of Io from its Occultation of β Scorpii C on May 14, 1971.
1091 *Icarus*, 17, 202–208
- 1092 Tsang, C. C. C., Spencer, J. R., Lellouch, E., Lopez-Valverde, M. A. and Richter, M. J., 2016. The collapse of Io's
1093 primary atmosphere in Jupiter eclipse. *Journal of Geophysical Research (Planets)*, 121, 1400–1410
- 1094 Tyler, R. H., 2008. Strong ocean tidal flow and heating on moons of the outer planets. *Nature*, 456, 770–772

- 1095 Vance, S. D., Panning, M. P., Stähler, S., Cammarano, F., Bills, B. G., Tobie, G., Kamata, S., Kedar, S., Sotin, C., Pike,
1096 W. T., Lorenz, R., Huang, H.-H., Jackson, J. M. and Banerdt, B., 2018. Geophysical Investigations of Habitability
1097 in Ice-Covered Ocean Worlds. *Journal of Geophysical Research (Planets)*, 123, 180–205. 1705.03999
- 1098 Veeder, G. J., Matson, D. L., Johnson, T. V., Blaney, D. L. and Goguen, J. D., 1994. Io's heat flow from infrared
1099 radiometry: 1983–1993. *Journal of Geophysical Research*, 99, 17095–17162
- 1100 Šebek, O., Trávníček, P. M., Walker, R. J. and Hellinger, P., 2019. Dynamic Plasma Interaction at Io: Multispecies
1101 Hybrid Simulations. *Journal of Geophysical Research (Space Physics)*, 124, 313–341
- 1102 Wamsteker, W., Kroes, R. L. and Fountain, J. A., 1974. On the Surface Composition of Io. *Icarus*, 23, 417–424
- 1103 Webb, T. W., 1871. Ueber die helligkeitsverhältnisse der jupiterstrabanten,. *Nature*, 4, 442–443
- 1104 Yoder, C. F., 1979. How tidal heating in Io drives the galilean orbital resonance locks. *Nature*, 279, 767–770
- 1105 Zahnle, K., Dones, L. and Levison, H. F., 1998. Cratering Rates on the Galilean Satellites. *Icarus*, 136, 202–222
- 1106 Zahnle, K., Schenk, P., Levison, H. and Dones, L., 2003. Cratering rates in the outer Solar System. *Icarus*, 163,
1107 263–289
- 1108 Zimmer, C., Khurana, K. K. and Kivelson, M. G., 2000. Subsurface Oceans on Europa and Callisto: Constraints from
1109 Galileo Magnetometer Observations. *Icarus*, 147, 329–347
- 1110 Zolotov, M. Y. and Fegley, B., Jr., 2000. Eruption conditions of Pele Volcano on Io inferred from chemistry of its
1111 volcanic plume. *Geophysical Research Letters*, 27, 2789–2792
- 1112 Zolotov, M. Y. and Shock, E. L., 2001. Composition and stability of salts on the surface of Europa and their oceanic
1113 origin. *Journal of Geophysical Research*, 106, 32815–32828

1114 **Recommended Reading**

- 1115 • *Jupiter: the planet, satellites and magnetosphere*, F. Bagenal, T.E. Dowling, and W.B. McKinnon, eds.. Cambridge planetary science series. Cambridge, UK: Cambridge University Press, 2004.
- 1116 • *Satellites of Jupiter*, D. Morrison, ed. The University of Arizona Press (Space Science Series), 1982.
- 1117 • *Europa*, R.T. Pappalardo and, W.B. McKinnon, eds. The University of Arizona (Space Science Series), 2009.
- 1118 • *Io After Galileo: A New View of Jupiter's Volcanic Moon*, R.M.C. Lopes J.R. Spencer, eds. Springer, 2006.
- 1119 • *Ganymede*, M. Volwerk, M. McGrath, X. Jia, T. Spohn, eds. Cambridge University Press, 2025.
- 1120